

The Neutron Environment  
Of A Cf-252 Facility

A Thesis

Submitted to the Graduate Faculty of the  
Louisiana State University and  
Agricultural and Mechanical College  
in partial fulfillment of the  
requirements for the degree of  
Master of Science

in

The Department of Nuclear Engineering

by

Robert Micheal Wyatt  
B.S., Louisiana State University, 1971

December, 1972

DEDICATED TO  
My loving wife, Jeanne

## ACKNOWLEDGMENT

Many people and groups have contributed to the progress of this work. Dr. John C. Courtney has been a tremendous help with his counsel and much needed encouragement. Dr. Frank A. Iddings was always willing to devote time to solve problems or to make instructive comments. Dr. Robert C. McIlhenny substantially contributed to this work in the areas of technical writing and the proper presentation of data. Dr. Myron H. Young has devoted many hours to reviewing and commenting on the technical aspects of this work. To these men I extend my deepest appreciation and gratitude.

The Radiation Shielding Information Center at Oak Ridge National Laboratory has been an invaluable aid in providing the computer codes and libraries to Louisiana State University. Special thanks are extended to Mr. Robert Roussin and Mrs. Margaret Emmett for their assistance and suggestions.

To Mr. Ernest Hamilton who aided in my familiarization with the IBM 360 computer system at LSU and to Mr. Lee Miller who aided in the construction phase of this work, I owe many thanks.

This work would not have been possible were it not for Dr. William F. Curry whose efforts resulted in my entry into the Nuclear Science Center. To this list I must add the United States Air Force and the Union Carbide Corporation whose programs and policies made this graduate study possible.

Last, but most important, I extend my deepest love, appreciation, and admiration to my parents, Frank and Elsie, and to my wife, Jeanne, for their years of encouragement, support, and sacrifice which have made my studies successful.

LIST

ABSTRACT

CHAPTER

I.

II.

III.

IV.

## TABLE OF CONTENTS

	PAGE
ACKNOWLEDGMENT .....	iii
LIST OF TABLES .....	vii
LIST OF FIGURES .....	viii
ABSTRACT .....	ix
CHAPTER	
I. Introduction .....	1
II. Theory of Monte Carlo .....	3
Introduction .....	3
Mathematical Background .....	4
The Boltzmann Transport Equation ....	12
Point-Detector Estimator .....	15
III. Principles of Discrete Ordinates .....	17
Discrete Ordinates in One-Dimension .....	17
Two-Dimensional Discrete Ordinates ..	19
IV. The Morse Code .....	21
The Random Walk Module .....	24
Multigroup Cross-Section Module .....	25
The Analysis Module .....	26
Geometry Module .....	29
Diagnostic Module .....	32
Program Picture .....	33
V. Design and Modeling of the Irradiation Chamber .....	35
Introduction .....	35
Chamber Design .....	37

	PAGE
Modeling of the Chamber.....	41
VI. Results and Recommendations .....	47
Recommendations .....	55
REFERENCES .....	57
APPENDIX A .....	59
APPENDIX B .....	64
APPENDIX C .....	69
VITA .....	77

## LIST OF TABLES

TABLE		PAGE
5-1	Nuclear Properties of Californium-252 .....	36
5-2	Californium-252 Neutron Source Spectrum in the 17-Group Structure Used in This Work .....	44
6-1	Calculated and Experimental Thermal Neutron Fluxes .....	49
6-2	Fast Flux Distribution Determined Experimentally .....	51
6-3	Comparison of DOT and MORSE Calculated Energy Spectra at the Center of the Chamber .....	52
6-4	Comparison of DOT and MORSE Calculated Energy Spectra at 4.0 cm. from the Center of the Chamber and Colinear with the Source .....	53
6-5	Comparison of DOT and MORSE Calculated Energy Spectra at the Inside Wall of the Chamber Colinear with the Source ....	54

## LIST OF FIGURES

FIGURE		PAGE
2-1	The Probability Density Function $f(x)$ (a) Unmodified Distribution (b) Modified Distribution .....	8
4-1	Hierarchy of Subroutines in the MORSE Code .....	23
4-2	Subroutines of the SAMBO Package Interfaced With a Typical Monte Carlo Program .....	28
4-3	Hierarchy of Subroutines in the General Geometry Package .....	31
5-1	Cutaway View of Cf-252 Irradiation Chamber .....	39
5-2	Source Stand for Use With Irradiation Chamber .....	40
5-3	Beta-Gamma Dose Rate As A Function of Time After a One-Hour Irradiation With a Ten Milligram Cf-252 Source .....	41
5-4	Modeling of Chamber System for DOT Code .....	43
5-5	Irradiation Chamber and Tank System Modeled for MORSE Geometry Input .....	46
6-1	Positions of Indium Foil Pairs Irradiated in the Chamber .....	49
6-2	Positions of Sulfur Vials Irradiated in the Chamber .....	51
A-1	Division of Zone 2,2,1 Into Blocks and Sectors for MORSE Input .....	63



## ABSTRACT

The objective of this work was to furnish the Louisiana State University Californium-252 Demonstration Center with a dry irradiation facility to increase irradiation capabilities. Calculations of the neutron flux distribution in this facility were made with the discrete ordinates code, DOT, and the Monte Carlo code, MORSE. These calculations were compared with the flux distributions measured by activation techniques.

The measured thermal fluxes and energy spectra agreed with the discrete ordinates calculations. However, the Monte Carlo calculations were high in low-energy groups and low in high-energy groups. This is a result of errors in the cross sections and inaccuracies in the handling program used to collapse the basic 100-group neutron cross sections to the less detailed structure used in the transport calculations.

This work has increased the capabilities of Louisiana State University by the addition of an irradiation chamber. Also, the MORSE Monte Carlo code is now operational on the LSU computer (an IBM 360/65) and should prove to be a valuable analytic tool.

## CHAPTER I

### INTRODUCTION

In the past three years californium-252 has become increasingly useful as an isotopic neutron source. Interest in this isotope has led the U.S. Atomic Energy Commission to establish a Californium-252 Demonstration Center at Louisiana State University. The function of the Cf-252 Demonstration Center is to stimulate interest and to provide facilities to develop applications for the radioisotope.

To maximize the utility of the demonstration center, a general-purpose irradiation chamber that could use the relatively high neutron fluxes generated by the Cf-252 is required. To maximize the utility of the chamber, both the neutron and gamma-ray fluxes should be well known as a function of position within it for any given source arrangement.

The objective of this thesis was to design, build, and experimentally and theoretically document the neutron and gamma-ray fluxes within a multipurpose irradiation chamber. The Multigroup Oak Ridge Stochastic Experiment (MORSE) code, a Monte Carlo computer package, and the Discrete Ordinates Transport (DOT) code, a discrete ordinates computer package, were employed in the theoretical treatment of the chamber.\*

DOT is a general purpose code which solves the linear,

---

\* Both computer packages were provided to LSU by The Radiation Shielding Information Center (RSIC), at the Oak Ridge National Laboratory (ORNL), in Oak Ridge, Tenn.

energy-dependent, Boltzmann transport equation for specialized two-dimensional geometries ( $r$ - $z$ ,  $r$ - $\theta$ , and  $x$ - $y$ ) by a finite difference technique known as discrete ordinates or Carlson's  $S_n$  method.<sup>(1)</sup> Previously at LSU, this code has been applied to the analysis of very subcritical systems of light water and natural uranium.<sup>(2)</sup> The MORSE code is a multipurpose neutron and gamma-ray stochastic code which uses the Monte Carlo calculational technique to solve the Boltzmann equation.<sup>(3)</sup> A feature that increases the versatility of the code is a general three-dimensional geometry package as well as specialized one- and two-dimensional geometry packages. Time dependence of radiation intensities can also be treated for reactor kinetics problems. Other features include an accurate treatment of anisotropic scattering, and an albedo option for both neutrons and gamma-rays at any material surface. RSIC provided a version of the code which was operable on the ORNL computer, an IBM 360/75/91; however, a major task of this thesis project was to make this code package operable on the LSU computer, an IBM 360/65. This involved coding changes because of compiler differences and the requirement at LSU for an overlay structure using the general geometry package. In addition, a supplement to the user's manual for MORSE was prepared as an aid to personnel using the LSU version of the MORSE package.

## CHAPTER II

### THEORY OF MONTE CARLO

#### Introduction

A reliable method for treating the transport of neutrons through matter is required in many areas of nuclear engineering. Criticality, shielding and many other calculational areas share this common need. Prior to the last decade, existing analytic and numerical methods for treating neutron transport were severely hampered by limitations placed upon the geometry, source distribution, and media characteristics. Often these limitations prevented or sorely compromised use of these methods in practical configurations.

A method which is essentially free from all these limitations is the Monte Carlo method.<sup>(4)</sup> The Monte Carlo method is a mathematical technique used to estimate a desired average quantity by random sampling from the probabilities describing the true stochastic process. The "stochastic process" refers to the phenomena in which quantities assume different values at different times and which may be represented as a family of random variables which fluctuate in time.<sup>(4)</sup> A Monte Carlo calculation may then be considered as the performance of an idealized experiment upon a system whose properties are known; that is, the sets of probabilities sufficient to describe the action of the system are known. The study is carried out using counters (represent-

ing detectors) of known resolution and absolute efficiency. Like most measurements involving counting, however, the Monte Carlo technique is subject to statistical errors. In practice, a balance must be reached between higher accuracy in statistics and higher computer costs which are necessary to achieve higher accuracy.

In the following sections of this chapter the mathematics of the Monte Carlo method and its application to solving the linear, energy-dependent Boltzmann transport equation, and flux-at-a-point estimation will be outlined.

#### Mathematical Background<sup>(4)</sup>

Random Numbers: Consider some independent variable,  $x$ , which assumes values over a specified interval  $(a,b)$ . Let  $\xi$  be any particular value of the independent variable; this variable will be referred to as the random variable of the independent variable  $x$ . A given physical situation will determine a set of probabilities that  $\xi$  assumes some particular value,  $x_1$ , or that  $\xi$  lies in some interval  $\Delta x_1$ .

A set of numbers over an interval such as  $(0.0,1.0)$  constitutes a set of random numbers if they are uniformly distributed over the interval and if no correlation exists within a randomly selected sequence of these numbers. A rigorous definition of the random number is that the probability of it being selected from an interval,  $y$ , contained in zero to one is  $y$ . In practice there exist computational algorithms adapted to digital computers that generate random numbers. However, these numbers are not truly random

and should more properly be called pseudo-random numbers. The period of such a distribution is the number of variables which can be chosen from the distribution before the sequence begins repeating itself. It is most important to ensure that the period of a pseudo-random number sequence is longer than the total number of random numbers which are required for a given calculation.

Probability Distributions: If  $\xi$  is a random variable of the independent variable  $x$ , then

$$F(x) = P(\xi \leq x) \quad (2-1)$$

is the probability that  $\xi$  is less than or equal to  $x$ . This function is defined for every  $x$  and is referred to as the cumulative distribution function (c.d.f.). The c.d.f. possesses the following properties:

- (1)  $F(x)$  is a non-decreasing function of  $x$ ,
- (2)  $F(x)$  is continuous from the right at a discontinuity,
- (3) If the variable  $x$  is a real number, then  $F(-\infty) = 0$  and  $F(+\infty) = 1$ ,
- (4) The probability that the random variable assumes a value within a finite interval  $(x_1, x_2)$  is given by

$$P(x_1 < \xi < x_2) = F(x_2) - F(x_1) \quad (2-2)$$

- (5) If the derivative  $dF(x)/dx$  exists at  $x$ , then for a small interval  $\Delta x$  about  $x$ , the probability that the random variable assumes a value within  $\Delta x$  is given approximately by

$$\lim_{\Delta x \rightarrow 0} P(x - \frac{\Delta x}{2} \leq \xi \leq x + \frac{\Delta x}{2}) \approx \frac{dF(x)}{dx} \Delta x . \quad (2-3)$$

The derivative of the c.d.f. is denoted as  $f(x)$  and is equal to the relative frequency of the random variable  $\xi$  per unit  $x$  about  $x$ . This function is called the probability density function (p.d.f.) of the independent variable  $x$ . Thus the p.d.f. is related to its corresponding c.d.f.

by

$$f(x) = \frac{dF(x)}{dx} \quad (2-4)$$

or by

$$F(x) = \int_{-\infty}^x f(x') dx'. \quad (2-5)$$

If  $f(x) = 0$  for all  $x < a$  and for all  $x > b$ , then  $f(x)$  must be a normalized function over the interval  $(a, b)$  :

$$\int_a^b f(x') dx' = 1 \quad (2-6)$$

where

$$F(a) = 0 \quad (2-6a)$$

$$F(b) = 1. \quad (2-6b)$$

Also, since  $F(x)$  is non-decreasing,  $f(x)$  must be non-negative on the interval  $(a, b)$ :

$$f(x) \geq 0 \quad a \leq x \leq b \quad (2-7)$$

Sampling Techniques: A very important phase of a Monte Carlo calculation is the selection of random variables according to the appropriate p.d.f. or related c.d.f. Consider two independent variables  $x$  and  $y$  and their corresponding distributions  $F(x)$  and  $G(y)$ . If the two c.d.f.'s have the same values, that is, if  $F(x) = G(y)$ , then  $\xi \leq x$  only if  $\eta \leq y$ . This follows because the c.d.f.'s are monotonically increasing functions. Therefore a distribution of random variables can be determined which conform to the c.d.f.  $F(x)$  if there

exists another c.d.f.  $G(y)$  such that

$$F(x_i) = G(y_i) \quad \text{for } i=1,2,3,\dots,N \quad (2-8)$$

Since random numbers can be generated with a computer very easily, a convenient choice for c.d.f.  $G(y)$  is the following:

$$\begin{aligned} G(y) &= 0 && \text{for } y \leq 0 \\ G(y) &= y && \text{for } 0 \leq y \leq 1 \\ G(y) &= 1 && \text{for } y \geq 1 \end{aligned} \quad (2-9)$$

The distribution  $G(y)$  is realized by the generation of numbers,  $R_i$ , uniform over the interval zero to one. The desired random variable,  $x_i$ , is calculated from

$$F(x_i) = \int_{-\infty}^{x_i} f(x') dx' = R_i \quad (2-10)$$

for  $i = 1, 2, \dots, N$

In principle, this approach to sampling yields a random variable,  $x_i$ , for each random number  $R_i$ . However, some difficulties may arise in the attempted execution of the inverse process,

$$x_i = F^{-1}(R_i). \quad (2-11)$$

As an alternative, the "rejection method" can be used, although it is less efficient since not all samples are used.

Consider the p.d.f.  $f(x)$  which is bounded on the interval  $(a,b)$ ; that is, it assumes some maximum value  $f(x_m)$  at  $x = x_m$  as shown in part (a) of Figure 2-1. Define a modified distribution function  $f_1(x)$  such that  $f_1(x_m) = 1$ ,

$$f_1(x) = f(x)/f(x_m), \quad (2-12)$$



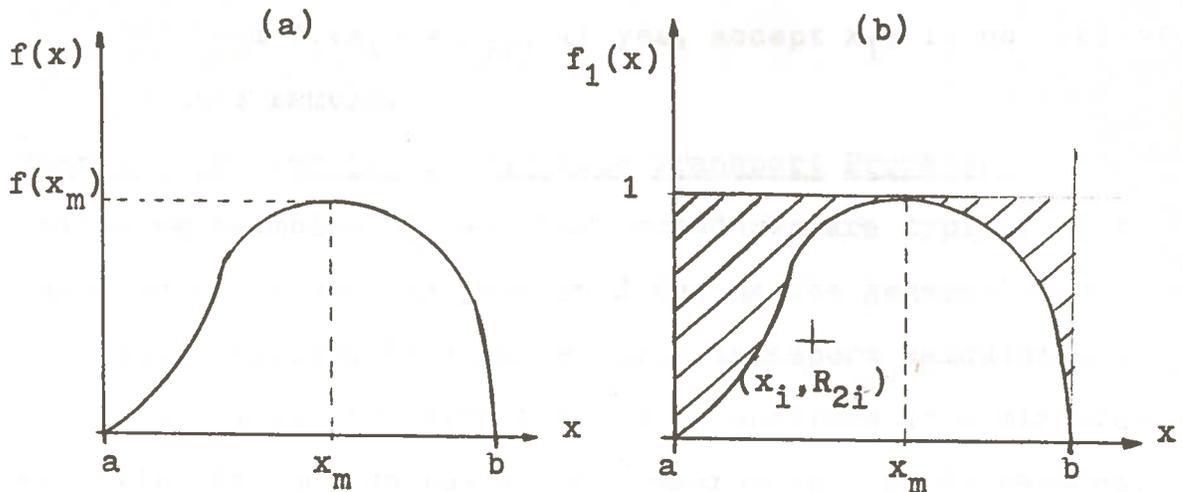


Figure 2-1. The Probability Density Function  $f(x)$   
 (a) Unmodified Distribution (b) Modified Distribution. (4)

and express the independent variable as

$$x_i = a + R_i (b - a) \quad (2-13)$$

where  $R_i$  is a random number from the computational algorithm. The procedure in the rejection method is to generate random numbers in pairs  $(R_{2i-1}, R_{2i})$  for each sample which is attempted. This combination is interpreted as defining a point  $\left[ a + R_{2i-1}(b-a), R_{2i} \right]$  with uniform probability of occurrence anywhere within the rectangle which circumscribes  $f_1(x)$  as shown in Figure 2-1(b). If the point falls under the curve  $f_1(x)$ , the sample is accepted and  $x_i$  is generated. If it falls above the curve (in the shaded area), the sample is rejected. So the procedure for the  $i$ th sample is the following:

(1) Select the random numbers  $(R_{2i-1}, R_{2i})$ .

(2) Calculate  $x_i$ ,

$$x_i = a + R_{2i-1} (b-a) \quad (2-14)$$

(3) Evaluate  $f_1(x_i)$ .

(4) Test  $f_1(x_i) \geq R_{2i}$ ; if yes, accept  $x_i$ ; if no, reject the sample.

Examples of Sampling in Particle Transport Processes: The following examples of sampling procedures are typical of the sampling which must be performed during the generation of a particle history in a Monte Carlo transport calculation.

(1) Select a nuclide from  $N$  kinds of nuclides in a mixture. Each kind of nuclide has a total macroscopic cross section,  $\Sigma_n$ , and the medium has a total macroscopic cross section,  $\Sigma_t$ , which is given by

$$\Sigma_t = \sum_{n=1}^N \Sigma_n . \quad (2-15)$$

Nuclide 1 is selected if a random number  $R$  is less than  $\Sigma_1/\Sigma_t$ , and the  $i$ th nuclide is selected if

$$\sum_{n=1}^{i-1} \frac{\Sigma_n}{\Sigma_t} \leq R < \sum_{n=1}^i \frac{\Sigma_n}{\Sigma_t} . \quad (2-16)$$

Once the nuclide has been selected, a choice must be made between an absorption or a scattering reaction. If another random number  $R$  is less than  $\Sigma_s/\Sigma_t$ , where  $\Sigma_s$  is the macroscopic scattering cross section, a scattering reaction will occur; otherwise, absorption occurs.

(2) Select the azimuthal scattering angle  $\phi$ , where its p.d.f. is given by

$$f(\phi) = 1/2\pi \quad (2-17)$$

Its corresponding c.d.f. is

$$F(\phi) = \int_0^{\phi} f(\phi') d\phi' = \phi/2\pi \quad (2-18)$$

and a value for  $\phi$  is obtained by setting

$$F(\phi_i) = R_i \quad (2-19)$$

where  $R_i$  is a random number; solving for  $\phi_i$  yields

$$\phi_i = 2\pi R_i \quad (2-20)$$

(3) Pick a distance from one collision site to the next.

the p.d.f. is given by

$$f(x) = \Sigma_t e^{-\Sigma_t x} \quad (2-21)$$

and the corresponding c.d.f. by

$$F(x) = \Sigma_t \int_0^x e^{-\Sigma_t x'} dx' = 1 - e^{-\Sigma_t x} \quad (2-22)$$

By letting

$$R_i = 1 - e^{-\Sigma_t x_i} \quad (2-23)$$

$x_i$  is given by

$$x_i = -\frac{1}{\Sigma_t} \ln(1-R_i) \quad (2-24)$$

Evaluation of Integrals By Monte Carlo Methods: When considering single or double integrals, normal numerical integration techniques give accurate results with less effort than with Monte Carlo methods, but for higher order multiple integrals, Monte Carlo becomes a practical tool.<sup>(5)</sup>

The Monte Carlo method can be demonstrated by the evaluation of the following integral:

$$I = \int_a^b g(x) \cdot f(x) dx \quad (2-25)$$

This integral generates the average of the function  $g(x)$  weighted by the p.d.f.  $f(x)$  over the interval  $(a,b)$ . This integral can also be expressed as

$$I = \int_0^1 g(x) dF(x) \quad (2-26)$$

where

$$F(x) = \int_a^x f(x') dx'. \quad (2-27)$$

The function  $F(x)$  is the c.d.f. corresponding to  $f(x)$ . With this transformation a selection of values of  $F(x)$  with uniform probability over the interval  $(0,1)$  is equivalent to selection of values of  $x$  according to  $f(x)$  over the interval  $(a,b)$ . The values of the random variable  $x$  are sampled from  $f(x)$  and for the  $i$ th random number,  $R_i$ , the  $i$ th selection of the random variable is given by

$$x_i = F^{-1}(R_i). \quad (2-28)$$

There is a corresponding value  $g(x_i)$ , and an estimation of the value of the integral is given by

$$\bar{I} = \frac{1}{N} \sum_{i=1}^N g(x_i), \quad (2-29)$$

where  $\bar{I}$  is the Monte Carlo estimate of  $I$  and  $N$  is an arbitrary number of samples.

When generalized to multidimensional integrals  $Q$ , over the multidimensional space  $P$ , the integral

$$Q = \iiint g(P) f(P) dP \quad (2-30)$$

is given by the Monte Carlo estimate  $\bar{Q}$ ,

$$\bar{Q} = \frac{1}{N} \sum_{i=1}^N g(P_i) \quad (2-31)$$

where the samples having space coordinates,  $P_i$ , are chosen according to a complex set of probabilities which generate the p.d.f.  $f(P)$ .

The Boltzmann Transport Equation (3)

The application of the Monte Carlo method to radiation transport becomes more evident if the Boltzmann transport equation is expressed in integral form. The derivation of the general time-dependent, integro-differential form of the Boltzmann transport equation can be regarded as a bookkeeping process that sets the storage of particles within a differential element of phase space ( $d\vec{r}, dE, d\vec{\Omega}$ ) equal to particle gains minus particle losses in the same differential element. This leads to the familiar and useful form

$$\begin{aligned} & \frac{1}{v} \frac{\partial}{\partial t} \phi(\vec{r}, E, \vec{\Omega}, t) + \vec{n} \cdot \vec{\nabla} \phi(\vec{r}, E, \vec{\Omega}, t) + \Sigma_t(\vec{r}, E) \phi(\vec{r}, E, \vec{\Omega}, t) \\ & = S(\vec{r}, E, \vec{\Omega}, t) + \iint dE' d\vec{\Omega}' \Sigma_s(\vec{r}, E' \rightarrow E, \vec{\Omega}' \rightarrow \vec{\Omega}) \phi(\vec{r}, E', \vec{\Omega}', t) \quad (2-32) \end{aligned}$$

where  $(\vec{r}, E, \vec{\Omega}, t)$  denotes the general seven-dimensional phase space coordinates:

$\vec{r}$  = the position variable,

$E$  = the particle's kinetic energy,

$v$  = the particle's speed corresponding to  $E$ ,

$\vec{\Omega}$  = the unit vector which describes the particle's direction of motion,

$t$  = time variable;

$\phi(\vec{r}, E, \vec{\Omega}, t)$  = the time dependent angular particle flux,

$\phi(\vec{r}, E, \vec{\Omega}, t) dE d\vec{\Omega}$  = the number of particles that cross a unit area normal to the direction  $\vec{\Omega}$  per unit time at the space point  $\vec{r}$  and time  $t$  with energies in  $dE$  about  $E$  and with directions within the solid angle  $d\vec{\Omega}$  about the unit vector  $\vec{\Omega}$ .

$\frac{1}{v} \frac{\partial}{\partial t} \phi(\vec{r}, E, \vec{\Omega}, t) dE d\vec{\Omega}$  = net storage per unit volume and time at the space point  $\vec{r}$  and time  $t$  of particles with energies in  $dE$  about  $E$  and with directions in  $d\vec{\Omega}$  about  $\vec{\Omega}$ ,

$\vec{\Omega} \cdot \nabla \phi(\vec{r}, E, \vec{\Omega}, t) dE d\vec{\Omega}$  = net convective losses per unit volume and time at  $\vec{r}$  and time  $t$  of particles with energies within  $dE$  about  $E$  and directions within  $d\vec{\Omega}$  about  $\vec{\Omega}$ ,

$\Sigma_t(\vec{r}, E)$  = the total cross section at the point  $\vec{r}$  for particles of energy  $E$ ,

$\Sigma_t(\vec{r}, E) \phi(\vec{r}, E, \vec{\Omega}, t) dE d\vec{\Omega}$  = collision losses per unit time and volume of particles at point  $\vec{r}$  with energies within  $dE$  about  $E$  and directions within  $d\vec{\Omega}$  about  $\vec{\Omega}$ ,

$\Sigma_s(\vec{r}, E' \rightarrow E, \vec{\Omega}' \rightarrow \vec{\Omega}) dE d\vec{\Omega}$  = the differential scattering cross section which describes the probability per unit path that a particle with an initial energy  $E'$  and an initial direction  $\vec{\Omega}'$  undergoes a scattering collision at  $\vec{r}$  which places it into a direction within  $d\vec{\Omega}$  about  $\vec{\Omega}$  and energy within  $dE$  about  $E$ ,

$\left\{ \iint \Sigma_s(\vec{r}, E' \rightarrow E, \vec{\Omega}' \rightarrow \vec{\Omega}) \phi(\vec{r}, E', \vec{\Omega}', t) dE' d\vec{\Omega}' \right\} dE d\vec{\Omega}$  = the in-scattering gains per unit volume and time at point  $\vec{r}$  and time  $t$  of particles of energies within  $dE$  about  $E$  and directions within  $d\vec{\Omega}$  about  $\vec{\Omega}$ ,

$S(\vec{r}, E, \vec{\Omega}, t) dE d\vec{\Omega}$  = source particles emitted per unit volume and time at point  $\vec{r}$  and time  $t$  with energies in  $dE$  about  $E$  and directions within  $d\vec{\Omega}$  about  $\vec{\Omega}$ .

A "quantity of interest" (denoted by  $\lambda$ ) such as bio-

logical dose, energy deposition, or particle flux for a given problem can be expressed in terms of the flux field  $\phi(\vec{r}, E, \vec{\Omega}, t)$  and an appropriate response function  $P(\vec{r}, E, \vec{\Omega}, t)$  due to a unit angular flux and is given by

$$\lambda = \iiint P(\vec{r}, E, \vec{\Omega}, t) \phi(\vec{r}, E, \vec{\Omega}, t) d\vec{r} dE d\vec{\Omega} dt . \quad (2-33)$$

For application to Monte Carlo, the energy dependence of equation (2-32) will be treated in terms of energy groups which are defined such that

$\Delta E_g$  = energy width of the gth group,

$g = 1$  corresponds to the highest energy group,

$g = G$  corresponds to the lowest energy group.

The group form of the Boltzmann equation expressed in terms of appropriate group parameters ( subscripted and superscripted with g's ) is the following:

$$\frac{1}{v_g} \frac{\partial}{\partial t} \phi_g(\vec{r}, \vec{\Omega}, t) + \vec{\Omega} \cdot \vec{\nabla} \phi_g(\vec{r}, \vec{\Omega}, t) + \Sigma_t^g(\vec{r}) \phi_g(\vec{r}, \vec{\Omega}, t) = S_g(\vec{r}, \vec{\Omega}, t) + \sum_{g' \neq g} \int_{4\pi} d\vec{\Omega}' \Sigma_s^{g' \rightarrow g}(\vec{r}, \vec{\Omega}' \rightarrow \vec{\Omega}) \phi_{g'}(\vec{r}, \vec{\Omega}', t) \quad (2-34)$$

By proper transformation of spatial coordinates, introduction of an integrating factor, and introduction of a quantity called "optical thickness"

$$\beta_g(\vec{r}, R, \vec{\Omega}) \equiv \int_0^R \Sigma_t^g(\vec{r} - R'\vec{\Omega}) dR' \quad (2-35)$$

where

$$R = |\vec{r} - \vec{r}'| \quad (2-36)$$

equation (2-34) can be transformed to the "Integral Flux Density Equation":

$$\phi_g(\vec{r}, \vec{\Omega}, t) = \int_0^\infty dR e^{-\beta_g(\vec{r}, R, \vec{\Omega})} \left[ S_g(\vec{r}-R\vec{\Omega}, \vec{\Omega}, t-R/v) + \sum_{g' \neq g} \int_{4\pi} d\vec{\Omega}' \Sigma_S^{g'}(\vec{r}-R\vec{\Omega}, \vec{\Omega}, \vec{\Omega}' \rightarrow \vec{\Omega}) \phi_{g'}(\vec{r}', \vec{\Omega}', t') \right] \quad (2-37)$$

If both sides of this equation are multiplied by  $\Sigma_t^g(\vec{r})$ , this becomes an expression for the event density  $\Psi_g(\vec{r}, \vec{\Omega}, t)$ , where

$$\Psi_g(\vec{r}, \vec{\Omega}, t) = \Sigma_t^g(\vec{r}) \phi_g(\vec{r}, \vec{\Omega}, t). \quad (2-38)$$

This represents the number of collision events per unit volume and time at point  $\vec{r}$  and time  $t$  experienced by particles having energies in the  $g$ th energy group and directions in  $d\vec{\Omega}$  about  $\vec{\Omega}$ .

The "Integral Event Density Equation" is of a reasonable form to be solved by the Monte Carlo technique. This equation is indeed the one that is chosen for the random walk in the MORSE code employed in this study. (10)

### Point Detector Estimator (6)

It is frequently desirable to use the Monte Carlo technique to estimate particle fluence, or some fluence-related quantity, at a point in space. One method of accomplishing this is to use a "next event" estimator which records from each collision point of a particle, the probability of the next event being at the point of interest.

The random walk process in a Monte Carlo code generates a sequence of collisions which are samples from the event density p.d.f.  $E(P)$  defined by the following:

$$E(P) = S(P) + \int E(P') K(P', P) dP' \quad (2-39)$$



where  $S(P)$  is the p.d.f. of particle births of particles with phase space coordinates  $P$ , and where  $K(P',P)$  is the conditional p.d.f. of events at  $P$ , given that the event originated at  $P'$ .

If  $S(P)$  and  $K(P',P)$  are given in terms of coordinates of particles entering an event (a collision or birth), the particle flux at the point  $\vec{r}$  can be expressed as

$$\phi(\vec{r}) = \iiint dE' d\vec{r}' dE d\vec{\Omega} * D(\vec{r}, E, \vec{\Omega}) * \left[ p\left(\frac{\vec{r}-\vec{r}'}{|\vec{r}-\vec{r}'|} \cdot \vec{\Omega}; E\right) \frac{e^{-\Sigma_t(E)|\vec{r}-\vec{r}'|}}{|\vec{r}-\vec{r}'|^2} \right] \quad (2-40)$$

where,

$D(\vec{r}, E, \vec{\Omega})$  = the density of particles entering collisions in a unit volume with energy in  $dE$  about  $E$  and direction in  $d\vec{\Omega}$  about  $\vec{\Omega}$  at the point  $\vec{r}$ ,

$p(\mu; E)$  = the probability per steradian of scattering a particle of energy  $E$  through an angle of  $\cos^{-1}\mu$ ,

$E'$  = energy of particles leaving the collision,

$\Sigma_t(E)$  = the total macroscopic cross section for particles of energy  $E$ .

Since the random walk process generates selections from the p.d.f.  $E(P)$ , a partial estimate of  $\phi(\vec{r})$  may be obtained by evaluating the quantity in square brackets in equation (2-40) for all collision sites.

## CHAPTER III

### PRINCIPLES OF DISCRETE ORDINATES

The discrete ordinates and other related methods of numerically solving the energy-dependent Boltzmann equation (Equation 2-32) have been used extensively in nuclear engineering. These methods have their foundation in the evaluation of the angular flux in a number of discrete directions instead of using an expansion in spherical harmonics or in Legendre polynomials. By considering enough discrete directions, it is possible, in principle, to obtain a solution to any desired degree of accuracy.

In discrete ordinates techniques, as in Monte Carlo techniques, the energy is also treated as discrete by treating the energy in arbitrarily selected groups. Also, the spatial dependence is treated in terms of a finite mesh spacing of space coordinates. Thus all independent variables in a time independent form of the transport equation are treated as discrete; hence the name -- discrete ordinates transport.

#### Discrete Ordinates in One Dimension

For a one energy group, steady-state treatment in slab geometry, the Boltzmann transport equation reduces to the following:

$$\mu \frac{\partial}{\partial x} \phi(x, \mu) + \Sigma(x) \phi(x, \mu) = \frac{C(x)\Sigma(x)}{2} \int_{-1}^{+1} \phi(x, \mu') d\mu' + S(x, \mu) \quad (3-1)$$

where  $\mu$  is the cosine of the scattering angle,  $\phi(x, \mu)$  is the angular dependent flux,  $\Sigma(x)$  is the macroscopic cross section, and  $C(x)$  is the mean number of particles emerging from collisions at  $x$ . By considering a discrete set of angles, the integral of the angular dependent flux can be expanded in a quadrature formula<sup>(3)</sup> with quadrature weights,  $w_i$ , such that

$$\int_{-1}^{+1} \phi(x, \mu) d\mu \approx \sum_{i=1}^N w_i \phi(x, \mu_i). \quad (3-2)$$

Substituting this into equation (3-1) yields a set of  $N$  coupled, first order differential equations for  $\phi(x, \mu_i)$

$$\mu_j \frac{\partial}{\partial x} \phi(x, \mu_j) + \Sigma(x) \phi(x, \mu_j) = \frac{C(x)\Sigma(x)}{2} \sum_i w_i \phi(x, \mu_i) + S(x, \mu_j),$$

for  $j = 1, 2, \dots, N$ . (3-3)

These equations can readily be solved by finite difference techniques once the boundary conditions and characteristics of the problem are specified.<sup>(7)</sup> The particular choice of weights and direction cosines affects the accuracy obtained in solving a given set of  $N$  equations. The set that is usually chosen is the Gaussian quadrature set which is widely applied in numerical integration.<sup>(8)</sup>

The first step in solving the system of equations (3-3) is to establish a mesh of spatial points, that is, of discrete values,  $x_k$ , where  $k = 0, 1, 2, \dots, K$  such that  $x_0$  corresponds to one boundary of the slab and  $x_K$  to the other. The resulting derivative terms can then be expressed as finite differences

$$\left. \frac{\partial}{\partial x} \phi(x, \mu_j) \right|_{x=x_{k+1/2}} \approx \frac{\phi(x_{k+1}, \mu_j) - \phi(x_k, \mu_j)}{x_{k+1} - x_k}, \quad (3-4)$$

where

$$x_{k+1/2} \equiv \frac{1}{2} (x_k + x_{k+1}). \quad (3-5)$$

This method can be applied to the set of equations (3-3) and then placed in suitable form to be solved by an iterative process, that is, beginning with some initial guesses for the  $\phi(x, \mu_j)$ 's and repeatedly solving the system of equations for a new set of fluxes until the solution set converges.

### Two-dimensional Discrete Ordinates

In curved geometries (spherical or cylindrical coordinates) the discrete ordinates treatment is complicated by the fact that the angular derivatives in the transport equation must also be approximated.<sup>(2)</sup> These derivatives arise in a curved geometry system because the velocity vector of a particle traveling in a straight line changes continuously.

In an analogous manner to that of the slab geometry treatment, the cylindrical geometry form of the energy dependent transport equation can be reduced to a set of difference equations. Consider a differential element of phase space in cylindrical coordinates,

$$dP = 2\pi r dr dz d\eta d\psi dE, \quad (3-6)$$

where  $\eta$  and  $\psi$  are angles describing the motion of a particle with energy  $E$ . A finite phase space cell,  $\Delta P$ , is defined as

$$\Delta P = \int_{r_i}^{r_{i+1}} \int_{z_j}^{z_{j+1}} \int_{\eta_k}^{\eta_{k+1}} \int_{\psi_n}^{\psi_{n+1}} \int_{E_g}^{E_{g+1}} 2\pi r dr dz d\eta d\psi dE \quad (3-7)$$

or

$$\Delta P = \pi(r_{i+1}^2 - r_i^2)(z_{j+1} - z_j)(\eta_{k+1} - \eta_k)(\psi_{n+1} - \psi_n)(E_{g+1} - E_g), \quad (3-7)$$

or

$$\Delta P = V_{I,J} \Delta \eta_K \Delta \psi_N \Delta E_G. \quad (3-8)$$

The lower case subscripts (i,j,k,n,g) refer to quantities evaluated at a surface of a finite phase space cell, and the upper case subscripts (I,J,K,N,G) refer to quantities which are defined for the cell as a whole. By applying a similar integration over a finite phase space cell to the cylindrical geometry form of the transport equation, the following difference equation is obtained:

$$\begin{aligned} & 2\pi \Delta z_J \bar{u}_D (r_{i+1} \phi_{G,i+1,J,D} - r_i \phi_{G,i,J,D}) + 2\pi \bar{r}_I \Delta r_I \bar{\eta}_D * \\ & (\phi_{G,I,j+1,D} - \phi_{G,I,j,D}) + \frac{\Delta z_i}{w_D} (\gamma_{n+1} \phi_{G,I,J,n+1,K} - \gamma_n * \\ & \phi_{G,I,J,n,K}) + V_{I,J} \Sigma_G^T \phi_{G,I,J,D} = V_{I,J} S_{G,I,J,D} + \\ & V_{I,J} \sum_{l=0}^L \sum_{m=0}^1 A_D^{l,m} \sum_{G'=1}^G S_{G,G'}^{1,m} \sum_{D'=1}^{NOA} A_{D'}^{l,m} \phi_{G',I,J,D} w_{D'}. \end{aligned} \quad (3-9)$$

The curvature coefficients,  $\gamma_n$ , are defined by

$$\gamma_n = \frac{1}{2} \Delta r_I \Delta \eta_K \xi_n = \frac{1}{2} \Delta r_I \Delta \eta_K \sqrt{1 - \eta_K^2} \sin \psi_n. \quad (3-10)$$

To make a unique solution possible, some additional conditions must be imposed on the flux. Some relationships between fluxes in adjoining cells will provide enough equations in this case. The set of equations used for this purpose are known as the "diamond difference" equations; these equations and their use are described in a work by Carlson. (9)

## CHAPTER IV

### THE MORSE CODE

The Multigroup Oak Ridge Stochastic Experiment (MORSE) code is a multipurpose neutron and gamma-ray transport Monte Carlo code.<sup>(3)</sup> MORSE has many features which allow a variety of options for the user, including the ability to treat neutron transport, gamma-ray transport, or coupled neutron and secondary gamma-ray production. MORSE also utilizes multigroup cross sections; allows solving either the forward or the adjoint problem; contains cross-section handling and analysis, general geometry or specialized one- and two-dimensional geometries, internal debugging routines, an ability to treat time dependence, and an albedo option at any material surface; and includes several types of importance sampling.

In the current work, MORSE is used in conjunction with the 100-group DLC2D library of ENDF/B nuclear data provided LSU by the Radiation Shielding Information Center (RSIC) at Oak Ridge National Laboratory (ORNL) at Oak Ridge, Tennessee.<sup>(10)</sup>

Of primary significance in the utility of MORSE is the structure of its functions into basic modules. Modules exist for input, geometry handling, transport analysis, cross-section handling, random-walk generation, and diagnostic aids. Each of these modules functions independently and can be interfaced with user-written modules which perform

similar functions.

Some distinguishing characteristics of MORSE compared to other Monte Carlo codes are its ability to treat an entire problem without the use of magnetic tapes, terminate a job internally after a set elapsed c.p.u. time and obtain an output of quantities based upon the number of histories treated up to that time, batch processing of particles for the purpose of determining statistics, and a repeat run feature which allows time dependent fission problems to be solved with statistical estimates. Also included in the output of MORSE are various counters which allow some insights into the physics of the interactions which are taking place.

Detailed descriptions of the subroutines used by MORSE and logical flow charts may be found in the work of E. A. Straker.<sup>(3)</sup> A complete description of the input necessary to describe a MORSE problem is found in Burgart.<sup>(11)</sup>

Figure 4-1 shows the hierarchy of the major subroutines in MORSE. With the aid of this figure, it is possible to see the functions of the various modules. INPUT initializes the arrays and variables necessary for the transport process. The initial calculations by the cross section module begin in subroutine XSEC. The analysis module of the code is interfaced with MORSE through subroutine BANKR. The analysis module makes use of the cross-section and geometry modules when making calculations of the "quantity of interest,  $\lambda$ ." With the exception of the output from the random walk process,

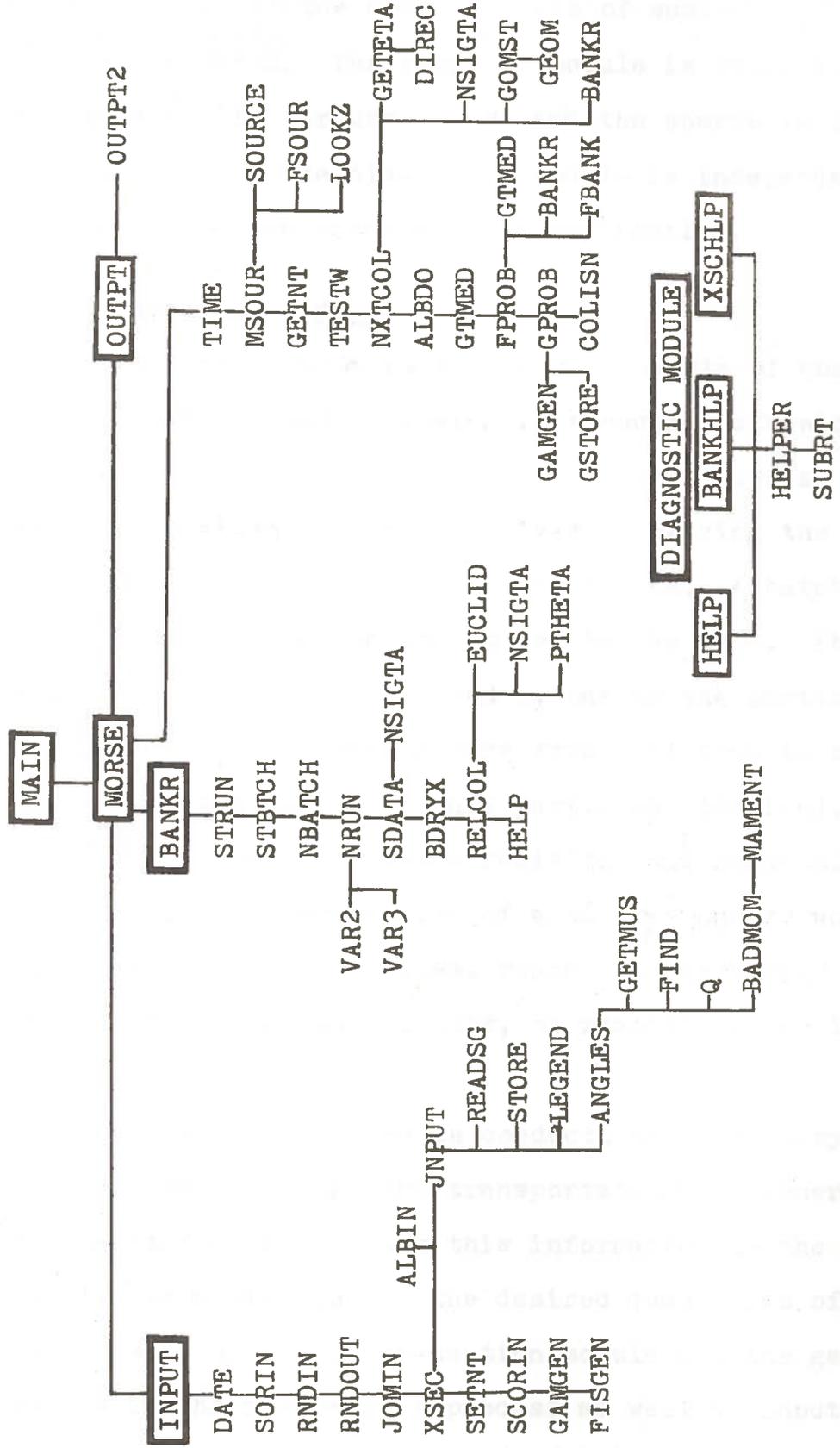


FIGURE 4-1. Hierarchy of Subroutines in the MORSE Code. (3)



the remainder of the code consists of subroutine calls from subroutine MORSE. The geometry module is interfaced with the analysis module through GOMST, and the source is interfaced through MSOUR. The diagnostic module is independent and any part of it may be executed from any routine.

### The Random Walk Module

The basic random walk process consists of choosing a source particle and following it through its history of events. This process is governed by the routines in this module. A given problem is solved by tracing the histories of a number of batches of such particles. A batch of source particles is generated and stored in the bank. The random walk of a batch is determined by taking the particles from the bank and transporting them from collision to collision, splitting particles into many particles (fission), killing (capturing) them by Russian roulette, and generating secondary particles. Termination of a history occurs when a particle leaks from the system, reaches a low energy cut-off, is killed by Russian roulette, or reaches an age limit (in time).

The random walk module conducts the necessary book-keeping for the bank, the transportation and generation of new particles, and relays this information to the analysis module for estimation of the desired quantities of interest. Use is made of the cross-section module and the geometry module in the random walk process as well as input and output routines for obtaining and printing information pertinent to

the problem.

After the necessary input operations and setting up of storage requirements, the walk process consists of three nested loops: one for runs, one for batches, and the innermost for particles. After each termination of the batch loop, bookkeeping is required before the generation of a new batch of source particles. After the termination of a run, a summary of the particle terminations, scattering counters and secondary production counters are output as well as results of Russian roulette and splitting for each energy group and region within the system.

#### Multigroup Cross Section Module

The function of this module in multigroup Monte Carlo codes is to read ANISN-type<sup>(12)</sup> cross sections for elements or media, mix several elements together to obtain media cross sections, determine group-to-group transfer probabilities, and determine the probabilities and angles of scattering for each group-to-group transfer. All variables within the code are flexibly dimensioned and are part of blank common (see Appendix A) storage. All types of cross sections may be treated by this module such as neutron only, gamma-ray only, neutron and gamma-ray coupled, or gamma-ray only from coupled neutron and gamma-ray input. Cross sections for either forward or adjoint solution of the Boltzmann equation may be obtained, and the Legendre coefficients for each group-to-group transfer may be retained for the next flight estimation.

After all cross sections are stored from input, the contribution of each element to the cross section for the medium is determined. Also at this time, the sum of the downscatter vectors for each group is determined for future calculation of the non-absorption probability. After the cross sections for the media have been determined, the non-absorption probability, fission probability, and gamma-ray production probabilities are formed by dividing the appropriate cross sections by the total cross section. The Legendre coefficients for each group-to-group transfer are converted to angles and probabilities of scattering at those angles by the use of a generalized Gaussian quadrature which uses the angular distribution as a weighting function. The use of this Gaussian quadrature is described in the work of E.A. Straker, et al.<sup>(3)</sup> These media cross sections, and the probabilities derived from them, are used in the random walk process to describe the transport of a particle through the system being treated.

#### The Analysis Module

SAMBO (Stochastic Analysis Machine for Bookkeeping)<sup>(6)</sup> is a package of computer routines which handles the drudgery associated with the analysis of collisions in a Monte Carlo code. SAMBO was specifically written for use with the MORSE code but should be readily adaptable for incorporation into other random walk generating codes. An arbitrary number of detectors, energy-dependent response functions, energy bins, time bins, and angle bins are allowed with virtually no

numerical limitations except the available core storage. Figure 4-2 is a simplified flow diagram of a typical Monte Carlo program interfaced with the SAMBO package. Input of parameters and initialization are performed at the beginning of each problem (SCORIN), each run (STRUN), and each batch (STBTCH). A batch is either a generation of particles in a multiplying system or a group of histories treated together for calculation of variances; a run is a set of batches. Terminal operations are performed at the end of each batch (NBATCH) and run (NRUN). The above mentioned routines, when called at the appropriate point by the history-generating routines, perform most of the necessary bookkeeping functions. Five additional routines are called by the primary bookkeeping routines or by the appropriate estimating routines: INSCOR and ENDRUN are dummies called by SCORIN and NRUN, respectively, to allow the user to make problem dependent modifications; VAR2 and VAR3 are called by NRUN to calculate fractional standard deviations in two- and three-dimensional arrays, respectively; and FLUXST is the interface between estimating and bookkeeping routines which is called by the estimating routines to store estimates in the proper arrays.

Many types of estimators are possible and no attempt is made to provide an all inclusive estimating routine. In lieu of this, a point-estimating routine is included by RSIC with the MORSE package. The method employed by this routine (described in Chapter 2) estimates the fluence at a point

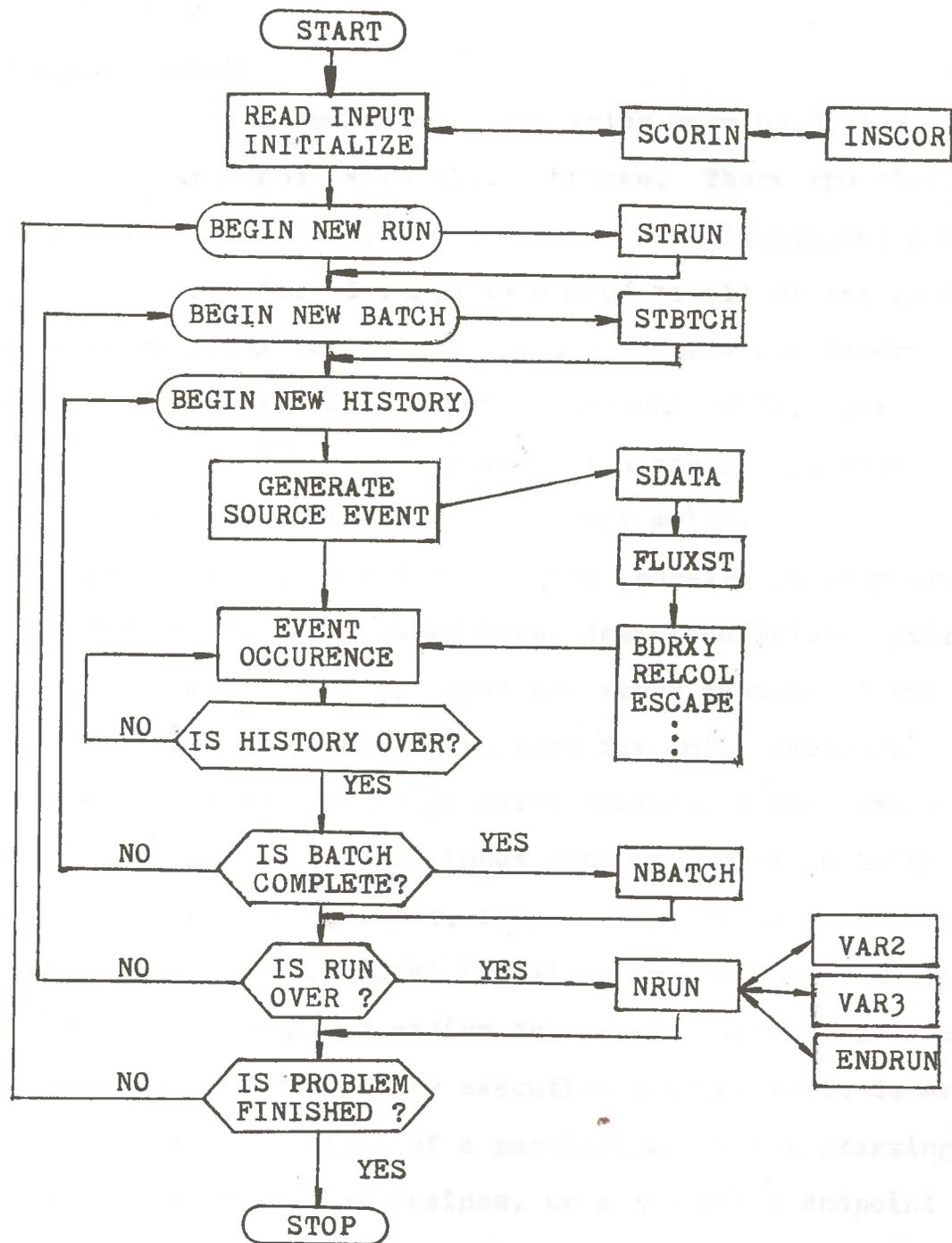


FIGURE 4-2. Subroutines of the SAMBO Package Interfaced With a Typical Monte Carlo Program.

detector.

### Geometry Module

MORSE uses geometry packages which were used with the  $\phi$ 5R Monte Carlo code with minor changes. There are slab, spherical, cylindrical, and general three-dimensional geometry packages available. Changes were made to all of the geometry packages to allow for albedo scattering from any material surface and for variable input and output units. The geometry packages may be replaced with special purpose geometry routines which the user might write.

The three main functions of the geometry package are performed by the three subroutines described below. Subroutine JOMIN reads geometry input and keeps account of the first location in blank common used for input geometry storage. In some special geometry packages blank common may not be used for storage of input data. Subroutine LOOKZ determines the block number, zone number, medium, and region for a point (x,y,z). LOOKZ is called from MSOUR to determine the starting region and medium for source particles. Subroutine GEOM is the primary executive routine which determines the endpoint of a flight of a particle given the starting point and the direction cosines, or a tentative endpoint and the number of mean free paths the particle will travel. It is called from GOMST and required information is obtained from a labeled common. In the more complicated geometry packages there are many routines which assist GEOM in determining the collision point.

The general three-dimensional geometry package is described in the  $\phi 5R$  code manual.<sup>(13)</sup> The only limitation in the detail which can be treated with this package is that all surfaces must be describable by quadratic equations in three-dimensional space. The description of the system must include a rectangular parallelepiped whose faces are parallel to the XY, YZ, and XZ coordinate planes. This parallelepiped is then divided into zones by planes which extend entirely across the system and which are parallel to the coordinate planes. The zones are divided into blocks by planes parallel to the coordinate planes but which extend only across the individual zones. Each zone is then divided into sectors by quadratic surfaces with a sector being defined by whether the volume is positive or negative with respect to the quadratic surfaces. Each sector may contain only one medium. Therefore, if a medium cannot be described by a single quadratic surface, it must be divided into several sectors. Besides material boundaries, both internal (medium 1000) and external (medium 0) void regions may be treated. An exterior void may be used in the exterior or the interior of the system. It behaves as a perfect particle absorber; that is, the particle is assumed to have escaped the system if it enters such a medium. An internal void is treated as transparent and particle paths are extended through it.

Figure 4-3 shows the hierarchy of subroutines in the general geometry package. Detailed descriptions of the

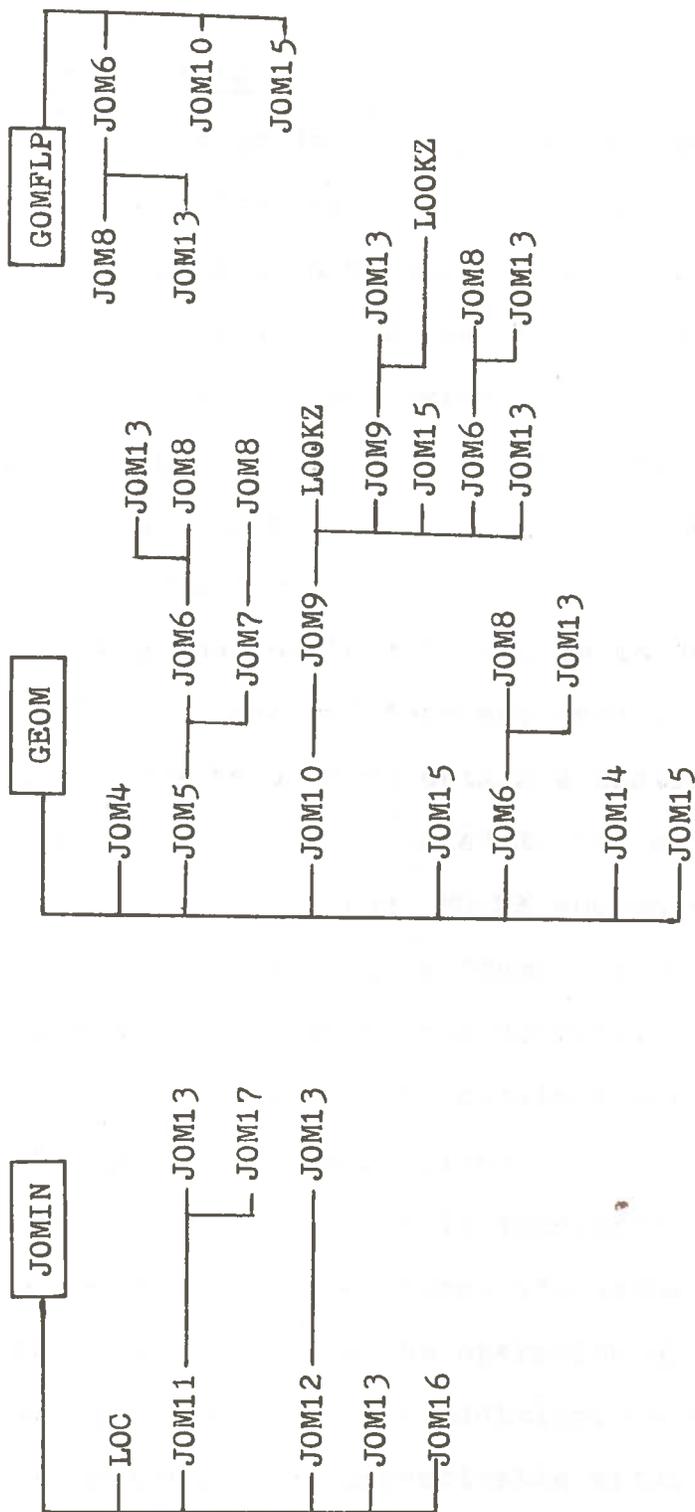


FIGURE 4-3. Hierarchy of Subroutines in the General Geometry Package. (3)



various subroutines used are given in the manuals which are available from RSIC. (13,3)

### Diagnostic Module

Frequently in debugging problem input parameters, or in trying to gain further insight into the physics of a problem, it is desirable to have the contents of some labeled commons or portions of blank common available for examination. The counters describing operations completed and interactions treated are stored in these common areas. The diagnostic module makes it possible to print, in a readable format, the values of these variables.

The key routine in this module is subroutine HELPER which prints in decimal form any part of a single precision array. HELPER is used to obtain a listing of appropriate common areas which are related to the situation of interest. HELPER is also called when MORSE encounters an unresolvable situation. The output is a "dump" of related common areas to facilitate location of the difficulty by the user. Subroutine HELP can be used to obtain a more inclusive dump of common areas if the need arises.

The diagnostic module is independent of all other modules of the MORSE code. Therefore, its debugging capability can be used at any point in the operation of the code that is desired by the user. In addition, automatic calls are made to this module if any unresolvable situation is encountered in the normal execution of a problem -- such as bad cross sections or incorrect geometry input data.

Program PICTURE<sup>(14)</sup>

The general geometry package has found wide usage in Monte Carlo transport codes. Because of GEOM's generality, preparing geometry input correctly is often a formidable task. GEOM itself can detect some of the errors and reject the input as written by the user. Frequently, however, an error cannot be determined by GEOM, because the input describes a perfectly legitimate geometry, but one that differs in some respect from that which was intended. To help the user determine whether or not the geometry input describes the geometry intended, a program called PICTURE was devised.

PICTURE displays, as a printed output, a representation of two-dimensional slices through the geometry as described by the input. A regularly-spaced array of points is generated and a call to GEOM determines the medium number at each of the points in the array. By printing out this array a relative picture of one view of the input geometry is produced. The user may visually inspect the picture and determine whether or not the geometry is as intended. By obtaining several such pictures of two-dimensional slices through the geometry, an overall picture of the geometry can be visualized.

PICTURE may be utilized in several different ways: an input parameter determines whether the output picture displays the material media or the region numbers. Input must also include the direction cosines of the axes of the two-

dimensional slice through the geometry. The area to be covered may then be specified by giving either the coordinates of the upper left and lower right corners of the picture, or by giving a starting point and the distances to be covered in the picture in each of the two axes' directions. By stacking input, several pictures may be obtained in a single run. If the picture is too large for a single printer page, it will then be continued on succeeding pages. These pages can then be separated and assembled in the proper orientation.

PICTURE is highly versatile and helpful to the user of the general geometry package accompanying the MORSE code. The input is simple -- consisting of six parameter cards in addition to the geometry input as prepared in the MORSE format. A more complete description of the input required and formats used may be found in the work of Irving and Morrison.<sup>(14)</sup>

## CHAPTER V

### DESIGN AND MODELING OF THE IRRADIATION CHAMBER

#### Introduction

In 1971 Louisiana State University was designated by the U. S. Atomic Energy Commission as a Californium-252 Demonstration Center. The demonstration center was to serve as a focal point for industry and educational institutions in the development of applications for californium-252, an isotopic neutron source. To accomplish this the AEC has made available through LSU various Cf-252 sources that range in size from one to 11,000 micrograms. Some of the nuclear properties of californium-252 are listed in Table 5-1. These properties make californium a highly versatile, isotopic neutron source.

To enhance the capability of developing applications of californium at LSU, several flexible facilities were built. The principal facility for the storage and use of sources is a four feet wide, eight feet long, and six and one half feet high tank of water, shielded on three sides by concrete blocks and borated sand. An assembly was built inside this tank so that samples could be irradiated in standard polyethylene vials. There was no provision, however, for the irradiation of samples which could not be placed in these vials. The irradiation chamber analyzed in the current work was proposed to increase the irradiation

PROPERTY	VALUE
Effective Half-life	2.646 years
Alpha Decay Half-life	2.731 years
Spontaneous Fission Half-life	85.5 years
Average Neutron Energy	2.348 MeV
Average Alpha Energy	6.117 MeV
Neutrons per Spontaneous Fission	3.76
Neutron Emission Rate	$2.34 \times 10^{12}$ n/sec-gm
Gamma Emission Rate	$1.3 \times 10^{13}$ photons/ sec-gm

TABLE 5-1. Nuclear Properties of Californium-252.

capability at LSU.

### Chamber Design

The objective of the current work was to design a useful, versatile, and inexpensive facility to extend LSU's capability to aid in the development of applications of californium-252. A general-purpose irradiation chamber for use with the cobalt-60 facility at LSU was already in existence. The same basic design concept used for that facility was adapted for the californium irradiation chamber; however, several different considerations had to be made because of the nature of the source to be used (that is, a neutron source as opposed to a gamma-ray source).

Factors which were considered in the design were the physical and nuclear properties of the chamber materials, sufficient size to facilitate a multipurpose chamber, and availability and cost of materials and labor. With these factors taken into account, a preliminary design using materials on hand and very simple construction techniques was conceived. It was then found that a piece of equipment was available which met the specifications then outlined for the chamber. This piece of equipment, a mixing tank for a liquid fuel rocket engine, was readily adaptable to the purposes at hand and saved a considerable amount of money and time.

The chamber consists basically of a right circular cylinder, weighted with lead at the bottom, and with a flange at the top. A top plate with an O-ring seal can be bolted

to the top of the cylinder's flange so that the chamber is air tight (see Figure 5-1). This provides a dry environment for specimen irradiations. The chamber was constructed of an aluminum alloy with a small percentage of magnesium. Fittings are available on the top of the chamber to facilitate many adaptations and modifications of the chamber (see Chapter VI).

In addition to the chamber, there was also a need for an apparatus to allow the placement of sources in a reproducible geometry with respect to the chamber. Because of the size and shape of the chamber, the existing source configurations were not readily adaptable. Thus, a new source holder was constructed of clear plastic (Plexiglass<sup>\*</sup>) for use with the chamber (see Figure 5-2). This source holder is considered a temporary facility because no attempt was made to optimize the source and chamber configuration. The source holder does, however, allow up to ten sources to be placed in a circular configuration around the chamber to achieve some uniformity of flux throughout it.

Because the chamber is constructed of aluminum and exposed to high neutron fluxes, there is a considerable amount of activation of the chamber itself. The  $\text{Al-27}(n,\gamma)$   $\text{Al-28}$  and  $\text{Al-27}(n,p)\text{Mg-27}$  reactions create a significant amount of activity in the chamber wall. The chamber was irradiated for one hour (essentially saturation for both

---

\*Registered trademark for acrylic sheet; Rohm and Haas Co.

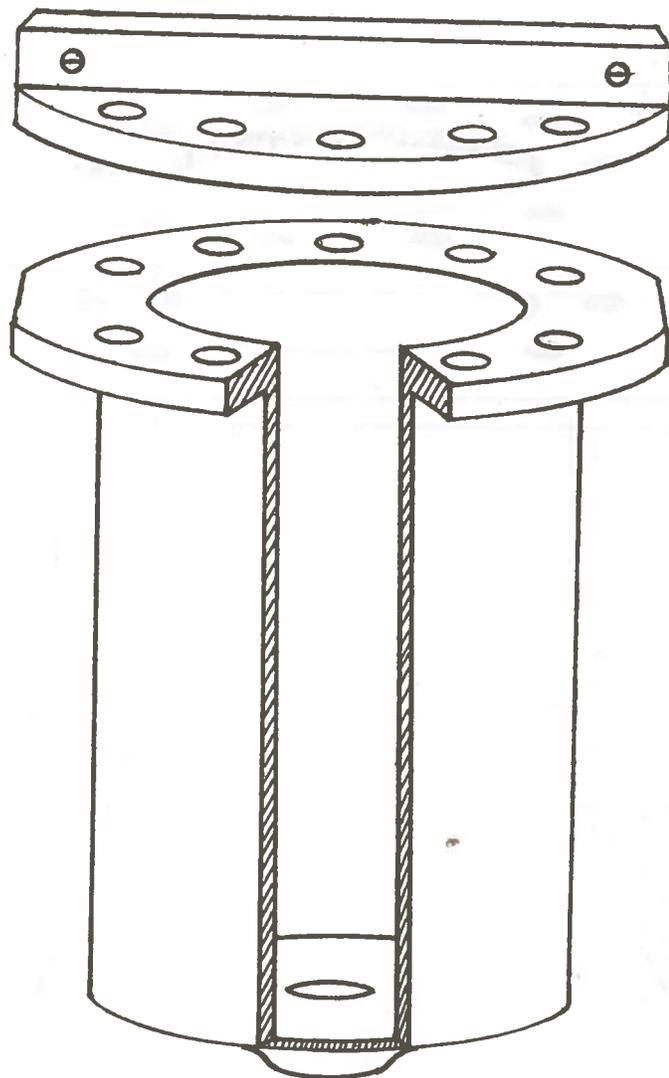


FIGURE 5-1. Cutaway View of Cf-252 Irradiation Chamber.



reactions) with a single ten milligram californium-252 source. The resulting beta-gamma dose rates at the surface of the chamber are displayed in Figure 5-3 as a function of decay time.

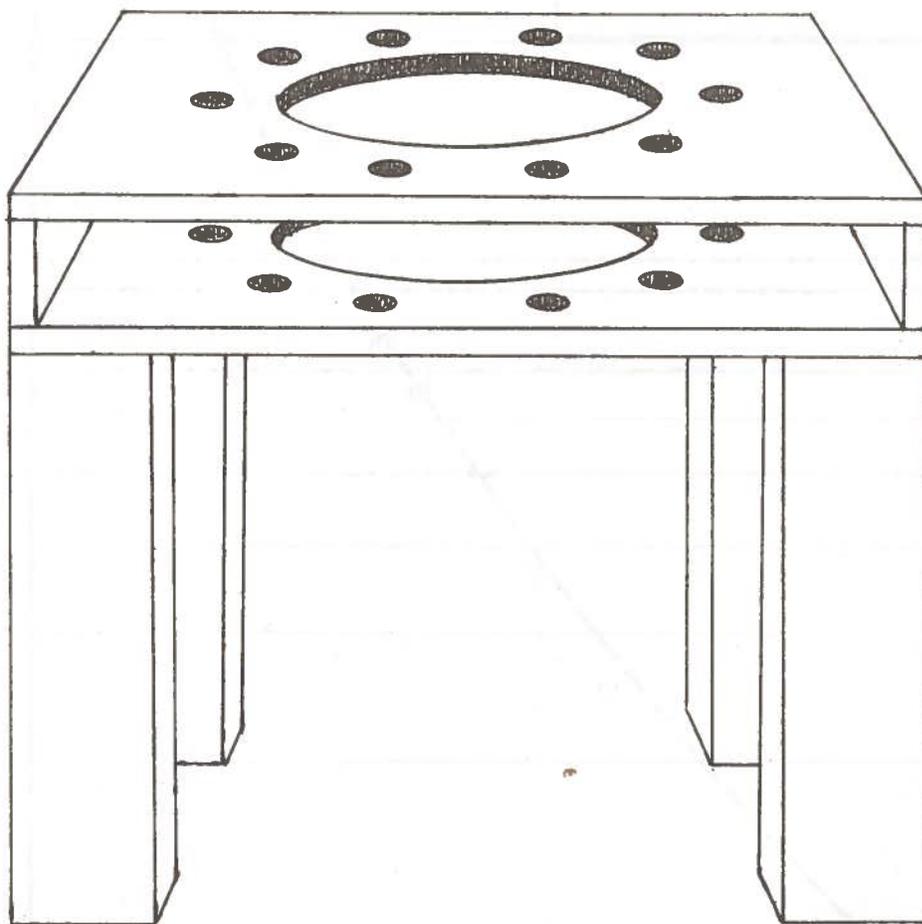


FIGURE 5-2. Source Stand for Use With Irradiation Chamber.

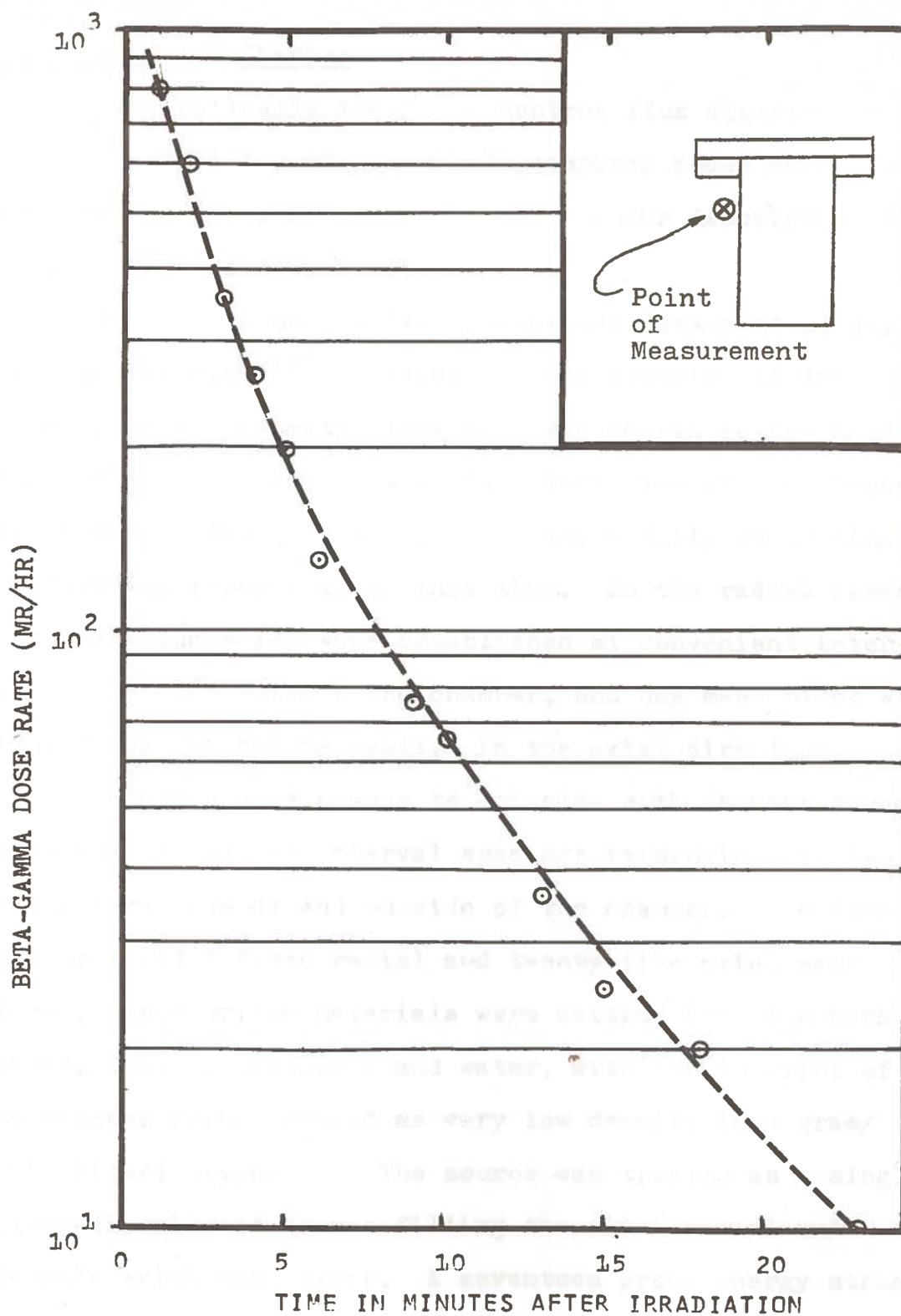


FIGURE 5-3. Beta-Gamma Dose Rate as a Function of Time After a One-hour Irradiation of the Chamber with a Ten Milligram Cf-252 Source.

### Modeling of the Chamber

To theoretically treat the neutron flux distribution in the chamber, the DOT and MORSE computer codes were used. The modeling necessary to adapt the chamber description to these codes is described below.

DOT performs only a two-dimensional treatment of any transport problem.<sup>(15)</sup> Because of the symmetry of the chamber, an r-z geometry treatment was chosen as the most applicable (see Figure 5-4). The centerline of the chamber was chosen as the axis of symmetry and a fully reflecting boundary was imposed along this line. In the radial direction mesh boundaries were established at convenient intervals inside and outside the chamber, and one mesh block was allowed for the chamber wall. In the axial direction, mesh boundaries were chosen to coincide with chamber boundaries and convenient interval spacings (approximately two centimeters) inside and outside of the chamber. The treatment utilized fifteen radial and twenty-five axial mesh blocks. Appropriate materials were entered into the mesh blocks, that is, aluminum and water, with the interior of the chamber being treated as very low density (one gram/cubic liter) oxygen. The source was treated as a single, volume-distributed source filling the sixth radial and eleventh axial mesh block. A seventeen group energy structure was employed in this treatment of neutron transport only (see Table 5-2). The source spectrum is normalized

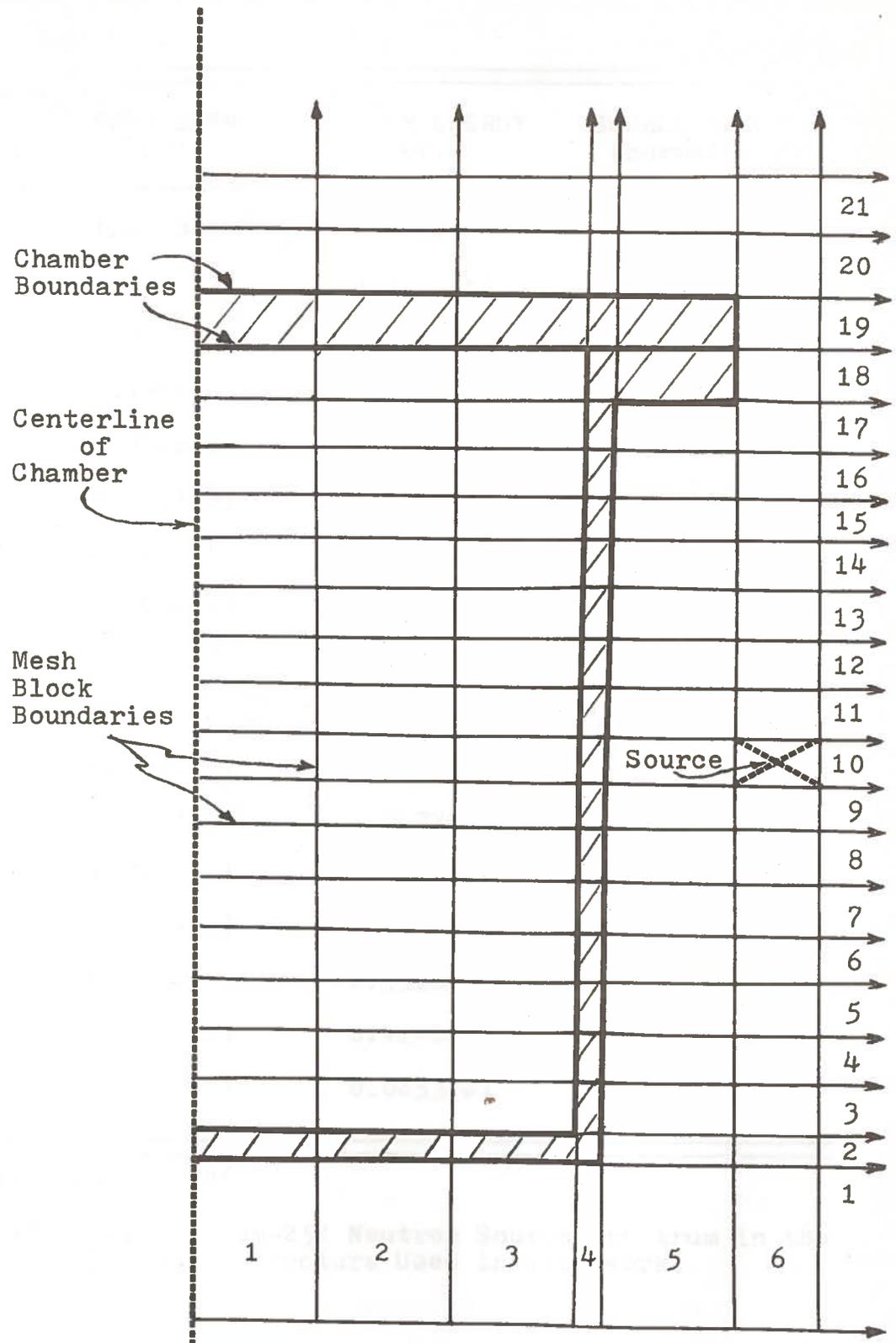


FIGURE 5-4. Modeling of Chamber System for DOT Code.

GROUP	UPPER ENERGY (ev)	LOWER ENERGY (ev)	SOURCE SPECTRUM (normalized)
1	1.4918(7) <sup>a</sup>	1.0000(7)	.00355
2	1.0000(7)	3.0119(6)	.27805
3	3.0119(6)	1.4957(6)	.32175
4	1.4957(6)	1.0026(6)	.14223
5	1.0026(6)	4.0762(5)	.17487
6	4.0762(5)	1.1109(5)	.06762
7	1.1109(5)	1.5034(4)	.01193
8	1.5034(4)	2.6126(3)	.00000
9	2.6126(3)	5.8295(2)	-
10	5.8295(2)	1.0130(2)	-
11	1.0130(2)	2.9023(1)	-
12	2.9023(1)	1.0677(1)	-
13	1.0677(1)	3.0509(0)	-
14	3.0509(0)	1.1254(0)	-
15	1.1254(0)	0.5316(0)	-
16	0.5316(0)	0.4140(0)	-
17	0.4140(0)	0.0253(0)	-

<sup>a</sup>Read as  $1.4918 \times 10^7$ .

TABLE 5-2. Californium-252 Neutron Source Spectrum in the 17 Group Structure Used in This Work.

to one neutron and collapsed from the 100-group spectrum for californium-252 provided with the DLC2D cross-section library by RSIC.<sup>(10)</sup>

Modeling for the MORSE code was somewhat more difficult and detailed than for the DOT code because of the three-dimensional geometry employed in MORSE. When in use, the chamber is placed in the four-feet by eight-feet by six-and-one-half-feet tank of water. This tank was taken as the system of interest for the MORSE treatment. This system model was surrounded by an external void (medium 0 in MORSE). The region interior to the tank was divided into three blocks (see Figure 5-5) with block boundaries as indicated to allow simple division of the chamber into sectors. The interior of the chamber was treated as an interior void (medium 1000 in MORSE). The geometric configuration used to treat the chamber and tank system required ten quadratic surfaces in addition to block and zone boundaries. For a complete listing of the geometry input see Appendix B.

The source was treated as a point fission source of neutrons using the Cf-252 spectrum of Table 5-2. The energy-group structure, fission spectrum, and cross-sections were the same as those for the DOT problem with the exception of the order of the expansion of the cross sections. A P-2 expansion was used in DOT with a later version of the DLC2D library,\* and a P-8 expansion was used in MORSE with an early version of the DLC2D library.

---

\*A corrected version of the July 1972 library issued October, 1972.

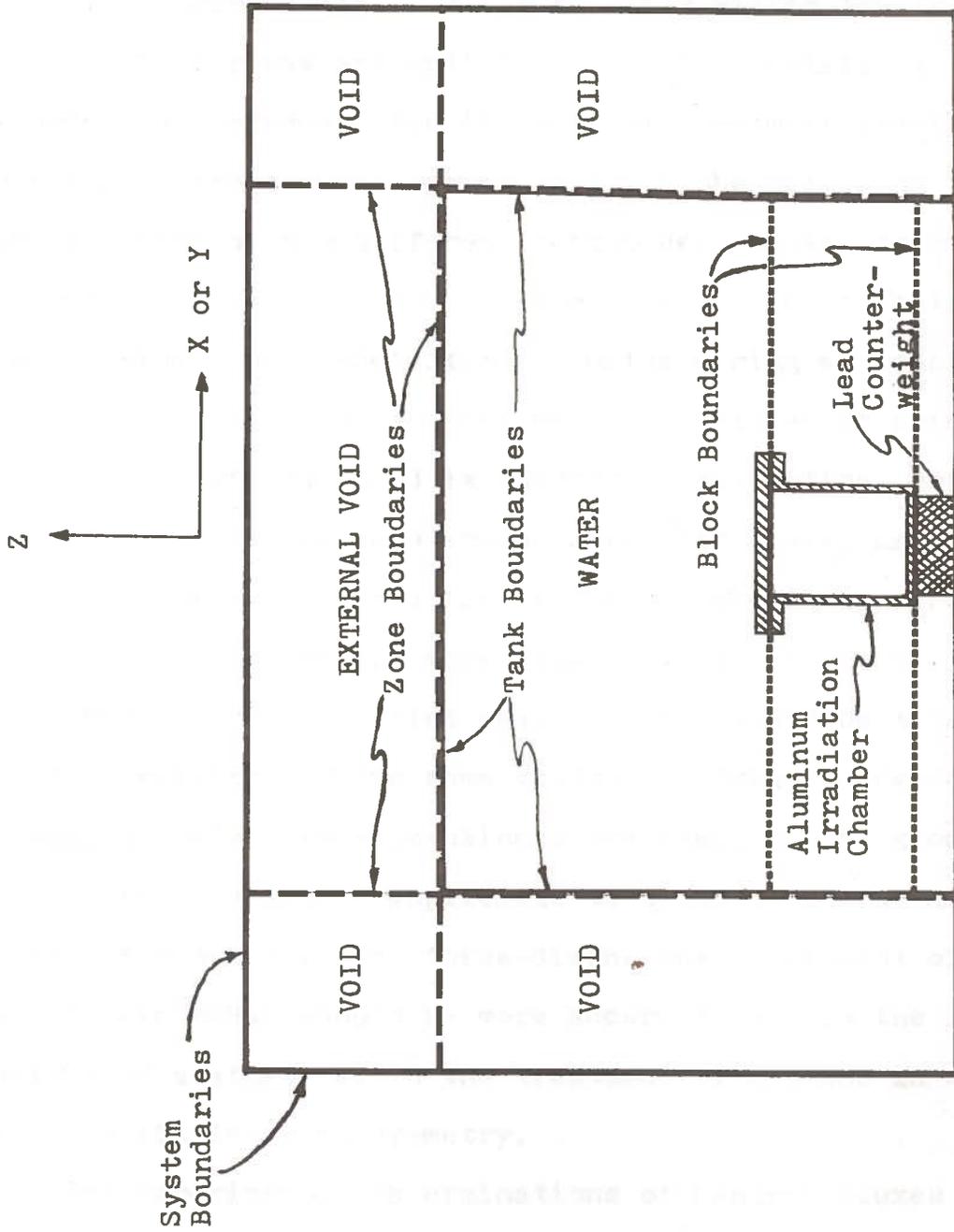


FIGURE 5-5. Irradiation Chamber and Tank System Modeled for MORSE Geometry Input.

## CHAPTER VI

### RESULTS AND RECOMMENDATIONS

The determination of neutron fluxes within the irradiation chamber was accomplished by both calculational and experimental methods. The theoretical treatment involved modeling of the chamber system to solve the Boltzmann transport equation by two different techniques, Monte Carlo and discrete ordinates. The MORSE Monte Carlo code calculates fluxes using a point-detector estimator during a stochastic experiment. The method of estimation of fluxes at points is somewhat difficult and is subject to statistical errors. The DOT discrete ordinates code solves for fluxes as average quantities over a finite phase space cell. The latter method is perhaps more applicable to the study of real systems, because point measurements cannot be made; all measurements involve some volume averaging. However, because of only a two-dimensional treatment of the geometry, this method may not be applicable to systems without a high degree of symmetry. The three-dimensional treatment of the geometry in MORSE should be more accurate, within the limitations of statistics, in the treatment of systems in which there is little or no symmetry.

The experimental determinations of neutron fluxes were made by standard activation techniques.<sup>(16)</sup> For thermal neutron flux determinations, bare and cadmium-covered indium



foils were used. The activity induced in these foils was measured with a 3" x 3" NaI(Tl) crystal and a multichannel analyzer by examining the 1.29 MeV gamma-ray which is characteristic of the decay of In-116m. Determinations were also made of the fast neutron flux (above 2.9 MeV) by using sulfur as a threshold detector. The S-32(n,p)P-32 reaction was used as the threshold reaction. The resulting P-32 activity (a pure beta emitter) was measured by liquid scintillation counting and comparison with a P-32 standard.

The positioning of indium foil pairs for thermal flux measurements within the chamber is shown in Figure 6-1. At each position a bare and cadmium-covered foil pair was placed and irradiated for about one half-life of In-116m (54.1 minutes). The results of these measurements (normalized to one source neutron) and the calculated values from DOT and MORSE are shown in Table 6-1.\* The thermal neutron fluxes for DOT and MORSE are those of group 17 of the energy structure (0.414 eV and below). This is a widely accepted range for the sub-cadmium flux. The general patterns of thermal neutron flux distributions are the same for both codes. The magnitude of the flux falls off as the distance from the source increases, and the fluxes at positions 4, 6, and 7 are approximately the same. The measured fluxes agree quite well with the calculational values from DOT, but are somewhat lower than the calculational values from MORSE. These differences can be attributed to several factors.

---

\* Numbers in parentheses are powers of ten.

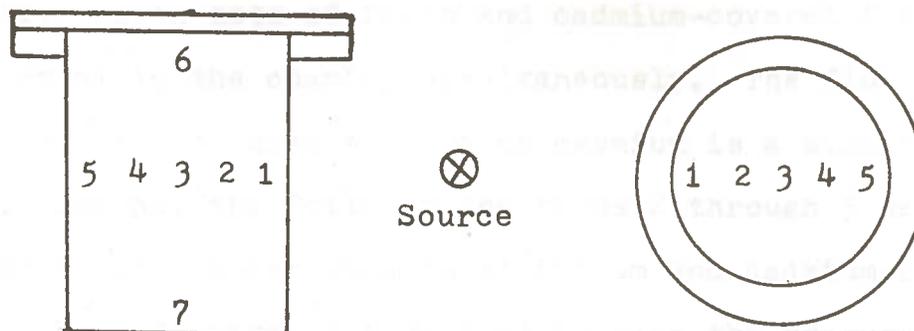


FIGURE 6-1. Positions of Indium Foil Pairs Irradiated in the Chamber.

POSITION	THERMAL NEUTRON FLUX PER SOURCE NEUTRON		
	MORSE	DOT	EXPERIMENTAL
1	$10.(-3) \pm 48\%$	$2.1(-3)$	$2.1(-3) \pm 30\%$
2	$5.8(-3) \pm 24\%$	$2.1(-3)$	$2.0(-3) \pm 30\%$
3	$4.7(-3) \pm 22\%$	$2.0(-3)$	$2.3(-3) \pm 30\%$
4	$3.9(-3) \pm 22\%$	-----	$2.5(-3) \pm 30\%$
5	$2.7(-3) \pm 31\%$	-----	$1.9(-3) \pm 30\%$
6	$4.4(-3) \pm 25\%$	$2.3(-3)$	$2.3(-3) \pm 30\%$
7	$3.7(-3) \pm 32\%$	$1.6(-3)$	$2.2(-3) \pm 30\%$

TABLE 6-1. Calculated and Experimental Thermal Neutron Fluxes.

First, all foils were irradiated simultaneously. Consequently, seven sets of foils and cadmium-covered foils were present in the chamber simultaneously. The flux depression due to large amounts of cadmium is a significant factor. Second, the foils in positions 2 through 5 were shadowed by increasing amounts of indium and cadmium-covered foils. Both of these factors tend to make the measured thermal fluxes lower than they would be in an unperturbed system. To alleviate these errors, a separate irradiation was conducted with only two foil pairs in the chamber at positions 1 and 7. Results from these measurements were used to normalize the remainder of the measurements. These are the results shown in Table 6-1.

In a separate irradiation, sulfur pellets and polyethylene vials of sulfur were placed into the chamber as threshold detectors for neutrons with energies above 2.9 MeV. The fluxes measured by this technique are shown in Table 6-2 for the positions within the chamber shown in Figure 6-2. These values are within the order of magnitude as calculated by DOT, but vary widely from those calculated by MORSE. The differences in the high energy group fluxes as calculated by DOT and MORSE at three points within the chamber can be seen by an examination of Tables 6-3 through 6-5. The MORSE values are several orders of magnitude lower than the DOT values which are in relative agreement with experimental values. These differences in calculated fluxes can be explained, in part at least, because of the different versions

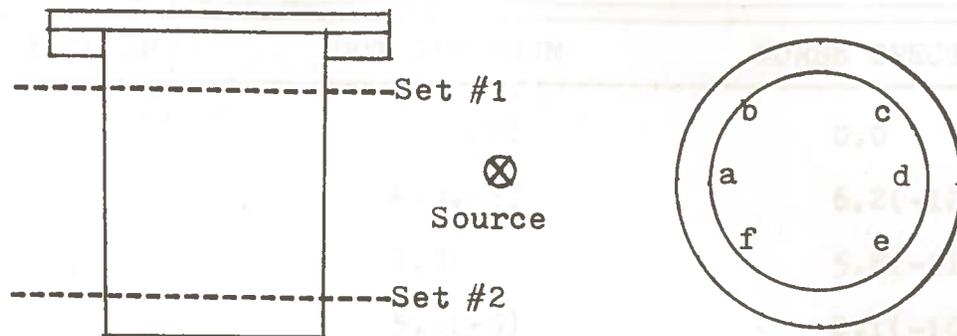


FIGURE 6-2. Positions of Sulfur Vials Irradiated in the Chamber.

POSITION	FAST NEUTRON FLUX (>2.9 MeV)
1a	1.4(-4)
1b	5.8(-5)
1c	3.0(-5)
1d	3.3(-5)
1e	4.1(-5)
1f	5.2(-5)
2a	2.5(-5)
2b	1.6(-5)
2c	1.5(-5)
2d	0.4(-5)
2e	1.2(-5)
2f	1.6(-5)

TABLE 6-2. Fast Flux Distribution Determined Experimentally.

ENERGY GROUP	DOT SPECTRUM	MORSE SPECTRUM
1	2.4(-7)	0.0
2	4.0(-5)	6.2(-12)
3	7.0(-5)	5.8(-11)
4	5.2(-5)	2.1(-10)
5	1.2(-4)	2.7(-10)
6	1.4(-4)	8.0(-10)
7	1.5(-4)	1.3(-9)
8	1.1(-4)	1.3(-8)
9	9.0(-5)	8.3(-8)
10	1.0(-4)	2.9(-7)
11	6.9(-5)	8.2(-7)
12	5.3(-5)	3.6(-6)
13	6.4(-5)	9.1(-6)
14	4.9(-5)	1.3(-5)
15	3.6(-5)	3.5(-5)
16	1.1(-5)	9.3(-5)
17	2.0(-3)	4.7(-3)

TABLE 6-3. Comparison of DOT and MORSE Calculated Energy Spectra at the Center of the Chamber.

ENERGY GROUP	DOT SPECTRUM	MORSE SPECTRUM
1	6.8(-7)	0.0
2	9.2(-5)	1.2(-11)
3	1.2(-4)	1.8(-10)
4	8.5(-5)	5.6(-10)
5	1.9(-4)	5.2(-10)
6	2.0(-4)	2.3(-9)
7	1.8(-4)	3.9(-9)
8	1.3(-4)	1.5(-8)
9	1.0(-4)	2.1(-7)
10	1.1(-4)	8.2(-7)
11	7.7(-5)	3.2(-6)
12	5.9(-5)	3.1(-6)
13	7.0(-5)	7.7(-6)
14	5.4(-5)	3.1(-5)
15	3.9(-5)	1.0(-4)
16	1.3(-5)	2.5(-4)
17	2.1(-3)	7.9(-3)

TABLE 6-4. Comparison of DOT and MORSE Calculated Energy Spectra at 4.0 cm. from the Center of the Chamber and Colinear with the Source.

ENERGY GROUP	DOT SPECTRUM	MORSE SPECTRUM
1	8.5(-6)	0.0
2	7.2(-4)	1.9(-11)
3	8.5(-4)	2.5(-10)
4	4.2(-4)	7.0(-10)
5	6.3(-4)	8.2(-10)
6	4.4(-4)	2.5(-9)
7	2.4(-4)	4.5(-9)
8	1.7(-4)	2.0(-8)
9	1.3(-4)	2.7(-6)
10	1.4(-4)	2.1(-6)
11	8.9(-5)	8.6(-6)
12	6.7(-5)	1.0(-5)
13	8.0(-5)	8.6(-6)
14	6.1(-5)	5.8(-6)
15	4.4(-5)	1.2(-4)
16	1.4(-5)	5.6(-4)
17	2.1(-3)	1.0(-2)

TABLE 6-5. Comparison of DOT and MORSE Calculated Energy Spectra at the Inside Wall of the Chamber Colinear with the Source.

of the cross sections used in these calculations.

In the cross-section module of MORSE, a non-absorption probability is calculated from cross-section input. For the high energy groups of lead, this probability was found to be greater than one. It is suspected that this is a result of inaccuracies in the code, APRFX-I, which was used to collapse the cross sections.<sup>(17)</sup> This non-absorption probability is used by MORSE in the flux-at-a-point estimator. So a high non-absorption probability and a low total macroscopic cross section resulted in a skewed energy distribution, away from higher energies and toward the lower energies. Because the total macroscopic cross section is in an exponential in MORSE and is a multiplicative factor in DOT, the DOT calculations were not affected in the same manner as the MORSE calculation.

### Recommendations

Some further work is still needed to make the irradiation chamber facility as useful as it could be.

First, further calculations using MORSE and DOT with cross sections collapsed by ANISN<sup>(13)</sup> or XCHEKR<sup>(3)</sup> instead of APRFX-I<sup>(10)</sup> may bring the two calculations into better agreement with themselves and with experiment. Second, the calculations and measurements were made with only one source. By employing superposition and the already measured and calculated fluxes, the distribution for a multiple-source configuration can be obtained. This would increase the utility of the chamber because of higher and more uniform fluxes.



Third, measurements of neutron and gamma-ray fluxes with thermoluminescent dosimeters (TLD's) have been estimated to yield probable errors of  $\pm 12\%$ . This would be a reasonable improvement upon the estimated accuracy of  $\pm 30\%$  for activation foil techniques.<sup>(18)</sup>

Fourth, the chamber may be modified or adapted to provide for many different types of studies. For example, the activation of gases may be studied with a flow-through system; and radiation effects upon operating electronic circuits may be observed. Other studies may be conducted on the effects of filter materials on the neutron spectrum within the chamber. This could lead to the optimization of the neutron energy distributions for various activation analyses.

The objective of the current work was to provide a useful chamber for larger scale irradiations with californium-252 sources with documented neutron and gamma-ray fluxes. Because of the lack of coupled neutron and gamma-ray cross sections and no adequate gamma-ray dosimetry system, the gamma-ray effort was not attempted in this thesis. However, with the documentation available on the thermal neutron distribution and the recommendations proffered for future uses, the chamber should be a useful addition to the facilities at the Louisiana State University Nuclear Science Center. The arsenal of computer codes at LSU has also been increased with the addition of the MORSE Monte Carlo code to the inventory.

## REFERENCES

1. P. N. Stevens and D. K. Trubey, Weapons Radiation Shielding Handbook. Chapter 3. "Methods for Calculating Neutron and Gamma-ray Attenuation", Defense Nuclear Agency Report Number DNA-1892-3, April, 1971.
2. E. L. Landry, "Discrete Ordinates Treatment of a Small Subcritical Assembly," M. S. Thesis, Louisiana State University, 1972.
3. E. A. Straker, P. N. Stevens, D. C. Irving, and V. R. Cain, "The Morse Code -- A Multigroup Neutron and Gamma-Ray Monte Carlo Transport Code," ORNL Report Number ORNL - 4585, Oak Ridge, Tennessee, September, 1970.
4. P. N. Stevens and D. K. Trubey, op. cit., pp. 27-36.
5. H. Kahn, "Random Sampling (Monte Carlo) Techniques in Neutron Attenuation Problems -- I and II," Nucleonics 6 (5), p. 27, and 6 (6), p. 60.
6. V. R. Cain, "SAMBO, A Collision Analysis Package for Monte Carlo Codes," ORNL Report Number ORNL - TM - 3203, Oak Ridge, Tennessee, September 1, 1970.
7. F. R. Mynatt, F. J. Muckenthaler, and P. N. Stevens, "Development of Two-Dimensional Discrete Ordinates Transport Theory for Radiation Shielding," ORNL Report Number CTC - INF - 952, Oak Ridge, Tennessee, August 11, 1969.
8. F. B. Hildebrand, Introduction to Numerical Analysis, (McGraw-Hill, New York, 1956).

9. B. G. Carlson, Numerical Solution of Neutron Transport Problems, "Proceeding of Symposium in Applied Mathematics, Volume XI", American Mathematics Society, 1961.
10. "100 Group Neutron Cross-Section Data Based on ENDF/B", ORNL Report Number DLC-2, Oak Ridge, Tennessee, July, 1972.
11. C. E. Burgart, "MORSE-GEOM-MORSEC-SAMBO Input Instructions", ORNL Report Number ORNL-TM-3632, Oak Ridge, Tennessee.
12. "ANISN, A One Dimensional Discrete Ordinates Transport Code", RSIC Manual Number CCC-82, Oak Ridge, Tennessee.
13. D. C. Irving, R. M. Freestone, Jr., and F. B. K. Kam, "Ø5R, A General-Purpose Monte Carlo Neutron Transport Code", ORNL Manual Number ORNL-3622, Oak Ridge, Tennessee, February, 1965.
14. D. C. Irving and G. W. Morrison, "PICTURE: An Aid In Debugging Geom Input Data", ORNL Report Number ORNL-TM-2892, Oak Ridge, Tennessee, May 14, 1970.
15. F. R. Mynatt, "A User's Manual for DOT", Union Carbide Nuclear Company, Report Number K-1694, January, 1967.
16. "Neutron Activation Foils", prepared by the Scientific Staff of Reactor Experiments, Inc., San Carlos, Calif.
17. Private communications with Robert Roussin, Radiation Shielding Information Center, Oak Ridge National Laboratory, Oak Ridge, Tennessee, April-November, 1972.
18. N. A. Hertelendy and J. C. Courtney, "Final Xe-Prime Dosimetry Report," Aerojet Nuclear Systems Co., August, 1970.

## APPENDIX A

## Supplement To MORSE User's Manual

The Fortran IV version of MORSE received by LSU was compatible with release 20.1 of the Fortran G compiler at LSU with one minor exception. The LSU system does not allow ending a do-loop with a statement which can transfer control, such as a LOGICAL IF statement. A simple remedy for this situation is to remove the statement number from the LOGICAL IF and place it on an inserted CONTINUE statement immediately following. This was the only Fortran language change that was necessary.

Other changes made to the MORSE package were made to the blank COMMON and were made for two reasons. First, the dimension of the blank common was 90,000 words. This dimension was much too large for the LSU system (IBM 360/65). There was no hope of fitting MORSE onto the LSU system because of a limit of 260,000 bytes of main storage with a four-byte word. The dimension of this common was, therefore, reduced to 26,000 words. This was more than adequate for the current work (19,500 words were used). Second, to allow for future use of hierarchy and low-speed core for this common block, blank common was changed to a labeled common, AMIKE. Therefore, there is no longer a blank common in MORSE; all commons are now labeled.

The routines of MORSE were compiled and placed as

three members of an object module library on disk. These object modules are input to the linkage editor by means of INCLUDE statements. Also input to the linkage editor is the OVERLAY structure which saves approximately 48,000 bytes and allows MORSE to be run in 246,000 bytes of main core. If hierarchy is employed at a future date, a region of (150K,110K) would be sufficient. Appendix B is a listing of the changes which were necessary to correct compilation errors and to incorporate changes such that hierarchy may be used without the need to recompile.

Appendix C contains a listing of the job control language (JCL), linkage editor input (the overlay structure), and the geometry input for MORSE. (Note: As of November 20, 1972, all data sets on disk used for DOT and MORSE have been catalogued and renamed under D7011.P50007.COURTNEY.)

The following are notes concerning specific points which may be of use to future users of the LSU version of MORSE:

1. Hierarchy of MORSE may be executed by the following:

```
// OS Job Card
```

```
//STEP1 EXEC FORTGC
```

```
//FORT.SYSIN DD *
```

(Subroutine ERROR -- User-written)

```
//STEP2 EXEC FORTGLG, PARM.LKED='HIAR,LIST,XREF,LET',
```

```
// REGION.GO=(150K,110K)
```

```
//LKED.MORSE DD DSN=D7011.P50007.COURTNEY.OBJECT,
```

```
// DISP=SHR
```

```
//LKED.SYSIN DD *
    INCLUDE MORSE(MAIN1)
    INCLUDE MORSE(MAIN2)
    INCLUDE MORSE(MAIN3)
    HIARCHY 1, AMIKE
    ENTRY MAIN
//GO.SYSIN DD *
    (MORSE Input Goes Here)
/*
//
```

2. Hierarchy and Overlay cannot be used simultaneously on an IBM 360.

3. The members of the object library and their contents are as follows:

MAIN1 -- SAMBO, MORSE, and Cross-Section Routines,

MAIN2 -- Library Functions and Machine Language  
Routines Necessary for MORSE,

MAIN3 -- Geometry Module and Subroutine BANKR.

4. Subroutine ERROR as used in this work is a dummy subroutine which writes a message saying that ERROR has been called. ERROR is provided for the user to write an error-handling routine to meet specific needs. ERROR is called whenever the diagnostic module is called during a MORSE run.

5. The geometry description in ORNL-4585 is probably insufficient for the user with no prior experience with MORSE input for the geometry module. A much more complete description is found in the Ø5R manual.<sup>(13)</sup> The geometry portion

of the input for MORSE for the chamber treated in this thesis is listed as a part of Appendix C (see also Figures A-1 and 5-5).

6. In the future, ANISN or XCHEKR is recommended for the cross-section collapsing with the DLC2D library.<sup>(17)</sup>

APRFX-I seemed to be inadequate.

7. To use program PICTURE, all subroutines in the geometry package as well as the following assembly language subroutines are necessary:

Subroutines AND, IAND, OR, IOR, ICOMPL, ERROR.

The assembly language routines are provided with MORSE. A copy of program PICTURE for general geometry is available from the Nuclear Science Center which includes all necessary subroutines.

8. The variable,  $RH\phi$ , in the mixing table is the atom density,  $N$ , times  $10^{-24}$ . The explanation of this on page of ORNL-4585 is somewhat confusing.

9. SURFACE and SECTOR cards in the geometry input must be omitted if the block contains only medium 0. (See Appendix C.)

10. The work of Burgart<sup>(11)</sup> is a complete description of the input for a MORSE problem and is strongly recommended as the source of information for the preparation of input.

11. If other problems are encountered in the use of MORSE, the personnel at RSIC are always willing to help. They may be contacted at phone 615-483-8611, extension 3-6944.

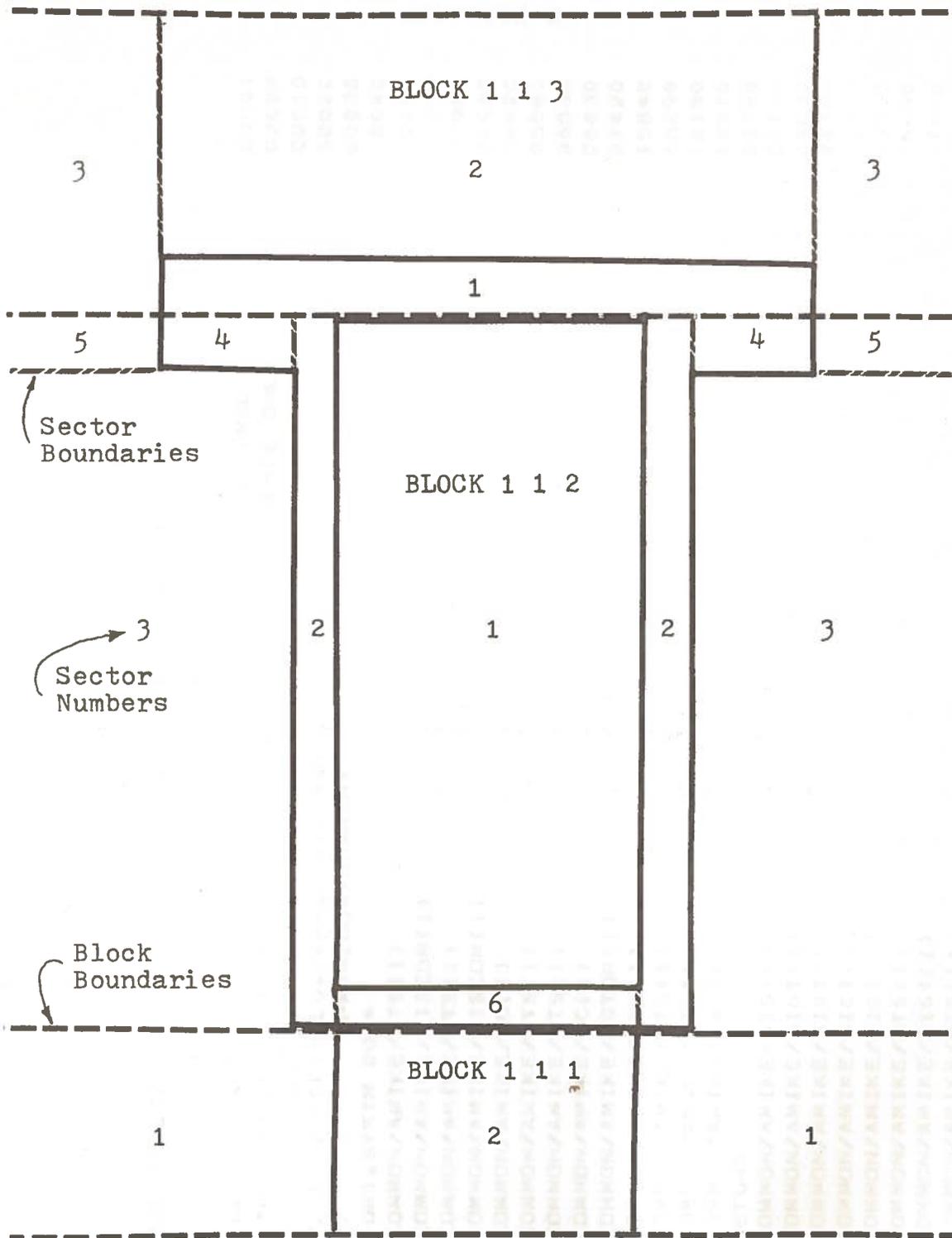


FIGURE A-1. Division of Zone 2 2 1 into Blocks and Sectors for MORSE Input.



APPENDIX B

C THE FOLLOWING CHANGES WERE MADE TO FILE NUMBER 1

C THE FOLLOWING JOB CONTROL LANGUAGE WAS ON THE ORIGINAL  
C TAPE LISTING. THEY ARE PROVIDED HERE FOR REFERENCE ONLY  
C // REGION.GO=470K  
C // EXEC FORTHCLG.PARM.FORT='MAP'.  
C // PARM.GO='DUMP=H'

C FORT.SYSIN DD \*  
COMMON/AMIKE/WTS(1)  
COMMON/AMIKE/FISCOM(1)  
COMMON/AMIKE/WTS(1)  
COMMON/AMIKE/FISCOM(1)  
COMMON/AMIKE/BC(1)  
COMMON/AMIKE/WTS(1)  
COMMON/AMIKE/WTS(1)  
COMMON/AMIKE/BC(1)  
COMMON/AMIKE/BC(1)  
COMMON/AMIKE/NSTOR(1)  
COMMON/AMIKE/VEL(1)  
COMMON/AMIKE/WTS(1)  
COMMON/AMIKE/WTS(1)  
COMMON/AMIKE/WTS(1)  
COMMON/AMIKE/NWTS(1)  
999 RETURN  
COMMON/AMIKE/SIGT(1)  
COMMON/AMIKE/SIGT(1)  
COMMON/AMIKE/SIGT(1)  
COMMON/AMIKE/SIGT(1)  
COMMON/AMIKE/SIGT(1)  
COMMON/AMIKE/SIGT(1)  
COMMON/AMIKE/WTS(1)  
COMMON/AMIKE/SIGT(1)  
COMMON/AMIKE/WTS(1)

00001  
00002  
00010  
00020  
00030  
00040  
00180  
03290  
03980  
04460  
04820  
05580  
06530  
06830  
07420  
15840  
16290  
18150  
19570  
21780  
22710  
24030  
24390  
25640  
25900  
26490  
27660  
33400

33750  
33920  
34770  
36250  
37110  
38760  
41130  
41640  
42170  
42380  
42381  
42640  
42641  
42910  
44360  
44361  
44660  
46350

C  
COMMON/AMIKE/WTS(1)  
COMMON/AMIKE/SIGT(1)  
COMMON/AMIKE/SIGT(1)  
COMMON/AMIKE/SIGT(1)  
COMMON/AMIKE/SIGT(1)  
COMMON/AMIKE/SIGT(1)  
COMMON/AMIKE/BL(1)

1 27H LAST LOCATION USED (PERM) ,I7 )

COMMON/AMIKE/BC(1)

IF (ICOMPA(BC(L),BC(M),4) .NE. 0) GO TO 25

15 CONTINUE

IF (ICOMPA(BC(L),BC(M),4) .NE. 0) GO TO 55

45 CONTINUE

COMMON/AMIKE/WTS(1)

IF (ICOMPA(A(L),A(M),4) .NE. 0) GO TO 45

35 CONTINUE

COMMON/AMIKE/NC(1)

COMMON/AMIKE/WTS(1)

THE FOLLOWING CHANGES WERE MADE TO FILE NUMBER 2

\*/ASSEMBLE.SYSIN DD \*

THE FOLLOWING CHANGES WERE MADE TO FILE NUMBER 4

\*/ASSEMBLE.SYSIN DD \*

00010

00010

C

C  
C  
C  
C  
C  
C  
\*  
C  
C  
C  
C  
C  
\*  
C

THE FOLLOWING CHANGES WERE MADE TO FILE NUMBER 9

C  
C  
C

COMMON / AMIKE / X	01060
COMMON / AMIKE / X	01950
COMMON / AMIKE / X	02730
COMMON / AMIKE / X	03570
COMMON / AMIKE / X	04250
COMMON / AMIKE / N	04470
COMMON / AMIKE / N	05040
COMMON / AMIKE / N(1)	05640
COMMON / AMIKE / X	06090
COMMON / AMIKE / N	06490
COMMON / AMIKE / X	06900
COMMON / AMIKE / X(1)	07450
41 CALL JOM15	08140
COMMON / AMIKE / X	08230
COMMON / AMIKE / X	10080
8050 FORMAT(1H , X2=,E12.4, Y2=,E12.4, Z2=,E12.4, X1=,E12.4, Y111	11000
1=,E12.4, Z1=,E12.4)	11010
COMMON / AMIKE / N(1)	11110

C  
C  
C  
C  
C

THE FOLLOWING CHANGES WERE MADE TO FILE NUMBER 10

COMMON / AMIKE / BC(1)	00750
COMMON / AMIKE / BC(1)	01330
COMMON / AMIKE / E(1)	02080
COMMON / AMIKE / BLNK(1)	05370
COMMON / AMIKE / BL(1)	08920

C THE FOLLOWING CHANGES WERE MADE TO FILE NUMBER 11

C  
C  
C

```

COMMON / AMIKE / NC(35000)
IF (NBK) 100,100,140
100 NBK = NBK + 5
GO TO (104,103,102,101),NBK
102 NBAT = NITS - ITERS
103 CALL NBATCH(NSAVE)
104 CALL NRUN(NITS,NQUIT)
140 GO TO (1,2,3,4,5,6,7,8,9,10,11,12,13),NBK
COMMON / AMIKE / VEL(1)
COMMON / AMIKE / BC(1)
COMMON / AMIKE / BC(1)
COMMON / AMIKE / EN(1)
COMMON / AMIKE / BL(1)
COMMON / AMIKE / EN(1)
COMMON / AMIKE / BC(1)
COMMON / AMIKE / NADD(12000)
COMMON / AMIKE / NADD(6000)
COMMON / AMIKE / NADD(6000)
COMMON / AMIKE / NC(35000)
COMMON / AMIKE / SIGT(1)
1 THROUGH ANGLE THETA PER STERADIAN FOR MEDIA *.13)
COMMON / AMIKE / WTS(1)
COMMON / AMIKE / WTS(1)
COMMON / AMIKE / VEL(1)
COMMON / AMIKE / VEL(1)

```

C  
C  
C

```

00040
00540
00550
00560
00600
00650
00680
00750
01130
03190
03590
03850
04220
04870
05210
06020
07050
07360
07840
08060
08460
09660
10020
11430
12410

```

THE FOLLOWING CHANGES WERE MADE TO FILE NUMBER 12

00040  
00770  
00780  
00790  
00830  
00880  
00910  
00980  
0155C

C  
C  
C

```

COMMON / AMIKE / NC(35000)
IF (NBANK) 100,100,140
100 NBANK = NBANK + 5
GO TO (104,103,102,101),NBANK
102 NBAT = NITS - ITERS
103 CALL NBATCH(NSAVE)
104 CALL NRUN(NITS,NQUIT)
140 GO TO (1,2,3,4,5,6,7,8,9,10,11,12,13),NBANK
1010 FORMAT(1H0,'ABCOS.GT.1. = ',E10.4)

```

THE FOLLOWING CHANGES WERE MADE TO FILE NUMBER 14

00040  
00430  
00740  
00750  
00760  
00800  
00850  
00880  
00950  
01320  
01660

C  
C  
C  
C  
C

```

COMMON / AMIKE / NC(35000)
COMMON / AMIKE / WTS(1)
IF (NBANK) 100,100,140
100 NBANK = NBANK + 5
GO TO (104,103,102,101),NBANK
102 NBAT = NITS - ITERS
103 CALL NBATCH(NSAVE)
104 CALL NRUN(NITS,NQUIT)
140 GO TO (1,2,3,4,5,6,7,8,9,10,11,12,13),NBANK
COMMON / AMIKE / EN(1)
COMMON / AMIKE / BC(1)

```

APPENDIX C

```

//ASMCCMP PROC
//ASM EXEC FGM=IEUASM,PARM=(LOAD,NODECK),REGION=100K,TIME=4
//SYSLIB DD DSN=SYS1.MACLIB,DISP=SHR
//SYSLT1 DD DSN=SYS1.SYSUT1,UNIT=SYSSQ,SPACE=(1700,(400,50),RLSE)
//SYSUT2 DD DSN=SYS1.SYSUT2,UNIT=SYSSQ,SPACE=(1700,(400,50),RLSE)
//SYSUT3 DD DSN=SYS1.SYSUT3,UNIT=SYSSQ,SPACE=(1700,(400,50),RLSE)
//SYSPRINT DD SYSCUT=A
//SYSFUNCH DD SYSCUT=E
//SYSGO DD CSN=LOADSET,UNIT=SYSSQ,DISP=(MOC,PASS),
//      SPACE=(800,(200,100),RLSE),DCB=BLKSIZE=800
//ENDPROC PEND
//LKED PROC
//LKED EXEC PGM=IEWL,PARM=(LET,XREF,LIST),REGION=96K,
//      CCND=(4,LT)
//SYSLIB DD DSN=SYS1.FORTLIB,DISP=SHR
//      DD DSN=SYS2.FORTLIB,DISP=SHR
//      DD DSN=SYS2.SSPLIB,DISP=SHR
//      DD DSN=SYS2.PLOTLIB,DISP=SHR
//SYSLMOD DD DSN=SYS2.GOSET(MAIN),UNIT=SYSDA,
//      DISP=(NEW,PASS),SPACE=(CYL,(6,1,1),RLSE),
//      CCE=BLKSIZE=7294
//SYSPRINT DD SYSCUT=A
//SYSUT1 DD UNIT=SYSDA,SPACE=(7294,(100,10),RLSE),
//      CCE=BLKSIZE=7294,DSNAME=SYSUT1
//SYSLIN DD DSN=LOADSET,UNIT=SYSSQ,DISP=(OLD,DELETE)
//      DD DDNAME=SYSIN
//ENDPROC FEND

```

```

//FCRTCCMP PROC
//FCRT EXEC PGM=IGIFORT,PARM='LOAD,NOTERM',REGION=100K,TIME=4
//SYSPRINT DD SYSCUT=A
//SYSPLUNCH DD SYSCUT=B
//SYSPLIN DD DSNNAME=&&LOADSET,UNIT=SYSSQ,DISP=(MOD,PASS),
// SPACE=(800,(200,100),RLSE),DCB=BLKSIZE=800
//ENDFROCC PEND
//GCPFROCC FRCC
//GC EXEC PGM=*STEP2.LKED.SYSLMOD,
// CCND=(4,LT)
//SYSDEL DD DSN=*STEP2.LKED.SYSLMOD,DISP=(OLD,DELETE)
//FT05F001 DD DDNAME=SYSIN
//FT06F001 DD SYSCUT=A
//FT07F001 DD SYSCUT=B
//ENDFROCC PEND
//STEP5 EXEC FCRTCCMP,REGION=100K
//FCRT.SYSIN DD *
SUBROLINE ERROR
WRITE(6,1)
1 FORMAT(1H1,'DEAR SIR,,//SX,'I REGRET TO INFORM YOU THAT A CALL HA
*S BEEN MADE TO ',//IX,'SUBROUTINE ERROR WHICH WAS NOT PROVIDED WITH
* THIS PACKAGE.,//EX,'YOU MUST NOW CALL OAK RIDGE AND GET A COPY OF
* THEIR LIBRARY VERSION OF THIS ROUTINE',//25X,'YOURS TRULY,,//25
*X,'MORSE')
RETURN
END
//STEP2 EXEC LKED,PARM,LKED='OVLY,LET,LIST,XREF'
//LKED.OBJECT DD CSN=D7011.P40C09.WYATT.OBJECT,UNIT=2314,
// DISP=(OLD,KEEP),V L=SER=LSU007
//LKED.SYSIN DC *

```

THE FOLLOWING IS THE OVERLAY STRUCTURE USED IN MORSE

```

INCLUDE OEJECT(MAIN1)
INCLUDE OEJECT(MAIN2)
INCLUDE OEJECT(MAIN3)
OVERLAY AA
INSERT INPUT
OVERLAY BE
INSERT SORIN,JOMIN,BKKNMC
INSERT JOM11,JOM12,JCM16
OVERLAY BE
INSERT ALEIN,JNFUT,XSEC,ANGLES,BACMCM,FIND,GETMUS,LEGEND
INSERT MAMENT,Q,READSG,STORE
OVERLAY BE
INSERT SCORIN,STRUN,INSCOR,ENRGYS
OVERLAY AA
INSERT SOURCE,GPROB,GETETA,EUCLID,FLUXST,ALBDC,GSTORE,DIREC,PTHETA
INSERT TESTW,NEATCH,STBTCH,FEANK,FPROB,GCMST,MSOUR,NXTCOL
INSERT CCLISN,GTICLT,GEOM,LOCKZ,NGRPL,GCMFLP
INSERT VAR3,NRUN,ENDRUN,VAR2
INSERT JOM4,JOM5,JCM9,JOM10,JM14
ENTRY MAIN

```



//STEP3 EXEC GOPRCC,REGICN.GO=260K,TIME.GO=019  
//GC.SYSIN CD \*

REGULAR MORSE INPUT GOES HERE

THE FOLLOWING IS THE GEOMETRY PORTION OF THE INPUT  
FOR DESCRIPTION OF THE CALIFORNIUM CHAMBER PROBLEM

2	MALE	MARRIED	
X ZCNES	-.10	C+11,-.	.1219D+03,.12192D+03,.10 D+11
Y ZCNES	-.10	D+11,-.	.6096D+02,.60960D+02,.10 D+11
Z ZCNES	0.0		.18288D+03,.10 D+11
ZCNE	1	1	
X BLOCK	-.10	C+11,-.	.1219D+03
Y BLOCK	-.10	C+11,-.	.6056D+02
Z BLCK	0.0		.18288D+03
BLCK	1	1	
MEDIA		0	
ZCNE	1	2	1
X BLOCK	-.10	C+11,-.	.1219D+C3
Y BLOCK	-.6096	C+02,	.60560D+02
Z BLCK	0.0		.18288D+03
BLOCK	1	1	1
MEDIA		0	
ZCNE	1	3	1
X BLOCK	-.10	D+11,-.	.1219D+03
Y BLOCK	.60960D+02,	.10	D+11

```

Z BLOCK      0.0      ,.18288D+03
BLOCK        1      1      1
MEDIA        0
ZCNE        2      1      1
X BLOCK     -.1219D+03,.12192D+03
Y BLOCK     -.10      C+11,-.6096D+02
Z BLOCK      0.0      ,.18288D+03
BLOCK        1      1      1
MEDIA        0
ZCNE        2      2      1
X BLOCK     -.1219D+03,.12192D+03
Y BLOCK     -.6096D+02,.60960D+02
Z BLOCK      .00000C+00,.66667D+01,.27932D+02,.18288D+03
BLOCK        1      1      1
MEDIA        1,      3
SURFACES    2
SECTOR +1
SECTOR -1
BLOCK        1      1      2
MEDIA       1000,    2,      1,      2
SURFACES    2,      3,      4,      5,      8
SECTOR +1   0      0      0      1
SECTOR -1  -1      0      0      0
SECTOR 0    1      0      -1      0
SECTOR +1   0      -1      1      0
SECTOR 0    0      1      1      0
SECTOR 0   -1      0      0      -1
BLOCK        1      1      1      3
MEDIA        2,      1,      1
SURFACES    4,      6,      9
SECTOR -1   0      -1

```

```

SECTOR -1 0 1
SECTOR 1 0 0
ZONE 2 3 1
X BLOCK -.1219D+03,.12192D+03
Y BLOCK .60960D+02,.10 D+11
Z BLOCK 0.0 ,.18288D+03
BLOCK 1 1 1
MEDIA 0
ZONE 3 1 1
X BLOCK .12192D+03,.10 D+11
Y BLOCK -.10 C+11,-.6096D+02
Z BLOCK 0.0 ,.18288D+03
BLOCK 1 1 1
MEDIA 0
ZONE 3 2 1
X BLOCK .12192D+03,.10 D+11
Y BLOCK -.6096D+02,.60960D+02
Z BLOCK 0.0 ,.18288D+03
BLOCK 1 1 1
MEDIA 0
ZONE 3 3 1
X BLOCK .12192D+03,.10 D+11
Y BLOCK .60960D+02,.10 D+11
Z BLOCK 0.0 ,.18288D+03
BLOCK 1 1 1
MEDIA 0
ZONE 1 1 2
X BLOCK -.10 D+11,-.1219D+03
Y BLOCK -.10 D+11,-.6096D+02
Z BLOCK .18288D+03,.10 D+11
BLOCK 1 1 1

```

MEDIA	0		
ZCNE	1	2	2
X BLOCK	-	.10	D+11, -.1219D+03
Y BLCK	-	.6096C+02, .60960D+02	
Z BLCK	.	.18288C+03, .10	D+11
BLOCK	1	1	1
MEDIA	0		
ZCNE	1	3	2
X BLOCK	-	.10	C+11, -.1219D+03
Y BLCK	.	.60960C+02, .10	D+11
Z BLCK	.	.18288C+03, .10	D+11
BLOCK	1	1	1
MEDIA	0		
ZCNE	2	1	2
X BLOCK	-	.1219C+03, .12192D+03	
Y BLOCK	-	.10	D+11, -.6096D+02
Z BLCK	.	.18288C+03, .10	D+11
BLOCK	1	1	1
MEDIA	0		
ZCNE	2	2	2
X BLOCK	-	.1219C+03, .12192D+03	
Y BLOCK	-	.6096C+02, .60960D+02	
Z BLOCK	.	.18288C+03, .10	D+11
BLOCK	1	1	1
MEDIA	0		
ZCNE	2	3	2
X BLOCK	-	.1219D+03, .12192D+03	
Y BLCK	.	.60960D+02, .10	D+11
Z BLOCK	.	.18288C+03, .10	D+11
BLOCK	1	1	1
MEDIA	0		

```

ZCNE      3      1      2
X BLCCK   .12192C+03,.10 D+11
Y BLCCK   -.10 C+11,-.60960D+02
Z BLCCK   .18288C+03,.10 D+11
BLOCK     1      1      1
MEDIA     0
ZCNE      3      2      2
X BLCCK   .12192C+03,.10 D+11
Y BLCCK   -.60960C+02,.60960D+02
Z BLCCK   .18288C+03,.10 D+11
BLOCK     1      1      1
MEDIA     0
ZCNE      3      3      2
X BLCCK   .12192C+03,.10 D+11
Y BLCCK   .60960C+02,.10 D+11
Z BLCCK   .18288C+03,.10 D+11
BLOCK     1      1      1
MEDIA     0

```

10 QUADRATIC SURFACES DESCRIBE CF 252 IRRADIATION CHAMBER

```

1.0      Z      -0.0      $
1.0      XSQ    +1.0      YSQ    -36.3919 $
1.0      XSQ    +1.0      YSQ    -43.4034 $
1.0      XSQ    +1.0      YSQ    -73.4884 $
1.0      Z      -27.145      $
1.0      Z      -27.932      $
1.0      Z      -6.6667      $
1.0      Z      -7.4604      $
1.0      Z      -28.732      $
1.0      Z      -182.88      $

```

## VITA

Robert Micheal Wyatt, born in Lafayette, Louisiana, on September 5, 1949, is the son of Mr. and Mrs. Frank L. Wyatt. After attending high school in Keyser, West Virginia, for three years, his family moved to Baton Rouge, Louisiana, where he graduated from Robert E. Lee High School in 1967.

He then entered Louisiana State University and received his Bachelor of Science degree in basic physics in May, 1971, and was commissioned as a second lieutenant in the U. S. Air Force. He was awarded a Union Carbide Corporation scholarship for graduate study. After completing the requirements for his bachelor's degree, he was called to active duty with the Air Force and assigned to the Civilian Institutions Program of the Air Force Institute of Technology and assigned to pursue a Master of Science degree in Nuclear Engineering at LSU.

Upon completion of this assignment at LSU he will be assigned to the Air Force Weapons Laboratory at Kirtland Air Force Base, New Mexico, as a nuclear research officer.